ANNUAL REVIEWS

Annual Review of Control, Robotics, and Autonomous Systems

Koopman Operators for Estimation and Control of Dynamical Systems

Samuel E. Otto and Clarence W. Rowley

Department of Mechanical and Aerospace Engineering, Princeton University, Princeton, New Jersey 08544, USA; email: cwrowley@princeton.edu

Annu. Rev. Control Robot. Auton. Syst. 2021. 4:59–87

First published as a Review in Advance on February 3, 2021

The *Annual Review of Control, Robotics, and Autonomous Systems* is online at control.annualreviews.org

https://doi.org/10.1146/annurev-control-071020-010108

Keywords

transfer operator, system identification, ergodic theory, dynamic mode decomposition, kernel methods, neural networks, stochastic systems

Abstract

A common way to represent a system's dynamics is to specify how the state evolves in time. An alternative viewpoint is to specify how functions of the state evolve in time. This evolution of functions is governed by a linear operator called the Koopman operator, whose spectral properties reveal intrinsic features of a system. For instance, its eigenfunctions determine coordinates in which the dynamics evolve linearly. This review discusses the theoretical foundations of Koopman operator methods, as well as numerical methods developed over the past two decades to approximate the Koopman operator from data, for systems both with and without actuation. We pay special attention to ergodic systems, for which especially effective numerical methods are available. For nonlinear systems with an affine control input, the Koopman formalism leads naturally to systems that are bilinear in the state and the input, and this structure can be leveraged for the design of controllers and estimators.

1. INTRODUCTION

The usual approach to modeling a dynamical system, with or without a control input, is to describe the evolution of the system's state. The state might be an element of a vector space (e.g., $\mathbb{R}^n$), a nonlinear manifold [e.g., SO(3)], or even a fractal set (e.g., a Cantor set), and one typically describes its evolution by means of an ordinary differential equation or a discrete-time map.

An alternative approach, common in ergodic theory, is to describe the evolution of functions on the state space. This approach is attractive for several reasons. First, even if the state lives on a manifold or a fractal set, the space of functions of the state is a linear space, often with additional structure such as an inner product. Furthermore, as observed by Koopman (1) in 1931, the evolution of functions is governed by a linear operator, which we now call the Koopman operator, so a wide array of tools from functional analysis are available. The utility of this approach was recognized immediately by von Neumann, who used it to prove the mean ergodic theorem (2), and this operator-based approach has been widely used in ergodic theory ever since.

Ergodic theory studies the steady-state behavior of systems after transients have decayed. For instance, after a long time, a system's state might approach a periodic orbit or chaotic attractor, and ergodic theory can characterize the dynamics on such invariant sets. In this setting, one can define a probability measure, which reflects the likelihood of finding the state in a given subset of state space. If there is such a probability measure that is invariant—that is, it does not change in time—then the system is called measure preserving. One then has a natural function space, such as the space of functions that are square integrable with respect to the probability measure. As we shall see, on this function space the Koopman operator acts isometrically (it preserves the norm), and its spectrum can tell us features about the long-term behavior, such as its mixing properties.

In many situations, especially for control, one is interested not only in the steady-state behavior of a system but also in its transient behavior. In fact, the objective of control is often to alter this transient behavior—for instance, to drive the state to a given point more quickly or to stabilize an unstable steady state. For such problems, the setting of ergodic theory does not seem immediately useful. However, these operator-based methods may also be used to study systems with transients. One loses some of the structure that is present in the measure-preserving setting (for instance, the Koopman operator is no longer isometric), but the spectrum of the Koopman operator can still give valuable information about a system's transient behavior.

Moreover, over the past two decades, several numerical methods have been developed to approximate the Koopman operator directly from data. These data-driven methods may be viewed as system identification methods and can provide models useful for analysis and control. Of course, these methods have advantages and disadvantages, and improving them is an active area of research. One of the main goals of this review is to provide an overview of the methods in use today and their strengths and weaknesses.

This review is organized as follows. In Section 2, we discuss the theoretical foundations of these operator-theoretic methods. We define the Koopman operator first in the context of measure-preserving systems and then generalize to other settings, such as stochastic systems and systems with transients. We show how the spectrum of the Koopman operator can be used to determine whether a system is chaotic (in the sense of mixing) and how eigenvalues and eigenfunctions may be used to define coordinates in which the dynamics are linear. In Section 3, we present methods for approximating the Koopman operator from data. In Section 4, we discuss methods for incorporating actuation into the Koopman operator framework and how the resulting models are useful for control and estimation. Finally, in Section 5, we offer some concluding remarks.

2. KOOPMAN OPERATOR METHODS: BACKGROUND

In this section, we define the Koopman operator, describe some of its properties, and illustrate its use on a few simple examples.

Observable: a complex-valued function on the state space

Consider a dynamical system that describes the evolution in time of a state variable x, which lies in some state space M. For the moment, we will consider a discrete-time dynamical system governed by

$$x(t+1) = Tx(t),$$

where $T : M \to M$ is a map, and t denotes time. We shall further assume that the state space M is a measure space; in particular, we have a probability measure μ that gives the size of (measurable) subsets of M, normalized so that $\mu(M) = 1$. We shall further assume that the map T is measure preserving.[1]

The Koopman operator acts on functions in the space $\mathcal{F} = L^2(M, \mu)$—that is, square-integrable functions of the state variable x.[2] In particular, for a function $f \in \mathcal{F}$, the Koopman operator $U : \mathcal{F} \to \mathcal{F}$ is defined by

$$Uf(x) = f(Tx). \tag{1.}$$

It is straightforward to see that, as long as T is measure preserving, the Koopman operator U is an isometry, since for any $f \in \mathcal{F}$, we have

$$\|Uf\|^2 = \int_M |f(Tx)|^2 \, \mathrm{d}\mu(x) = \int_M |f(y)|^2 \, \mathrm{d}\mu(T^{-1}y) = \int_M |f(y)|^2 \, \mathrm{d}\mu(y) = \|f\|^2,$$

where the third equality holds because T is measure preserving. If the map T is invertible, then U is unitary; otherwise, it is merely an isometry.

The Koopman operator allows us to understand a dynamical system by studying the linear operator U. This approach has several advantages; since the space $\mathcal{F}$ has some nice structure (it is a Hilbert space), we may use ideas such as linearity and orthogonality, and we can even study the spectrum of U.[3] By contrast, we have assumed little about the state space M. For instance, M may not even have the structure of a vector space or a smooth manifold; in fact, often it is a complicated fractal set, such as a chaotic attractor of a dynamical system.

One way to use the Koopman operator to gain insight about a dynamical system is to study its eigenvalues and eigenfunctions, or more generally its spectrum. For instance, suppose $\varphi \in \mathcal{F}$ is an eigenfunction of U, with eigenvalue $\lambda = e^{i\theta}$. (For a measure-preserving system, eigenvalues of U must lie on the unit circle, since U is an isometry.) Then we may define a coordinate or observable $z(t) = \varphi(x(t))$, and the evolution of this coordinate is particularly simple:

$$z(t+1) = \varphi(x(t+1)) = \varphi(Tx(t)) = U\varphi(x(t)) = \lambda\varphi(x(t)) = \lambda z(t). \tag{2.}$$

Thus, the coordinate z is decoupled from the other coordinates, and its evolution is even linear. Furthermore, since $|\lambda| = 1$ (for a measure-preserving system), the magnitude of z is constant along a trajectory, and its dynamics are simply a rotation by an angle θ.

Note that the constant function $f(x) = 1$ is always an eigenfunction of U, with eigenvalue 1, since $Uf(x) = f(Tx) = 1 = f(x)$ for all x. If the constant function is the only eigenfunction

[1] A map T is measure preserving if, for any measurable subset A, $\mu(T^{-1}A) = \mu(A)$.

[2] The Koopman operator may also be defined on other spaces, such as other L^p spaces, but here we confine ourselves to the L^2 setting.

[3] The spectrum is the set of $\lambda \in \mathbb{C}$ such that $U - \lambda I$ does not have a bounded inverse; if λ is an eigenvalue, then $U - \lambda I$ is not one to one, so λ is in the spectrum of U.

corresponding to eigenvalue 1, then the system is called ergodic.[4] If the system is ergodic, then the ergodic theorem says that for any function $f \in \mathcal{F}$ and almost every point $x \in M$,

Point spectrum: the set of all eigenvalues of an operator

$$\lim_{n\to\infty} \frac{1}{n}\big(f(x) + f(Tx) + \cdots + f(T^{n-1}x)\big) = \int_M f \, d\mu,$$

or, in other words, a function's time average equals its average over the state space. Intuitively, ergodicity means that, given enough time, almost all points will explore the whole state space. It also follows that if φ is an eigenfunction for an ergodic system, then $|\varphi(x)|$ is constant almost everywhere.

2.1. Example with Pure Point Spectrum: Rotation on a Circle

As an example, consider the state space $M = [0, 1)$, with Lebesgue measure, and dynamics given by

$$Tx = x + \alpha \pmod 1.$$

If we view x as a point on the unit circle [via the association $x \mapsto \exp(2\pi i x)$], then these dynamics simply rotate the point x through an angle $2\pi\alpha$. It is clear that the map T preserves Lebesgue measure.

Let us look at the eigenvalues and eigenfunctions of the Koopman operator U, which acts on functions in $\mathcal{F} = L^2(M)$. For each $n \in \mathbb{Z}$, consider the function $\varphi_n \in \mathcal{F}$ given by $\varphi_n(x) = \exp(2\pi i n x)$. Then,

$$U\varphi_n(x) = \varphi_n(Tx) = \exp\big(2\pi i n(x+\alpha)\big) = \exp(2\pi i n\alpha)\varphi_n(x),$$

so φ_n is an eigenfunction of U with eigenvalue $\lambda_n = \exp(2\pi i n\alpha)$. In this case, the spectrum of U consists entirely of eigenvalues, and the eigenfunctions φ_n form an orthonormal basis for $\mathcal{F}$. We then say that U has pure point spectrum.

If α is rational, then the number of distinct eigenvalues is finite. For instance, if $\alpha = 1/4$, then the eigenvalues are ± 1 and $\pm i$, and the eigenfunctions corresponding to the eigenvalue $+1$ are φ_0, $\varphi_{\pm 4}, \varphi_{\pm 8}, \ldots$. Because the constant function φ_0 is not the only eigenfunction corresponding to the eigenvalue $+1$, the system is not ergodic.

However, if α is irrational, then there are a countably infinite number of distinct eigenvalues, and they are dense on the unit circle. In this case, the constant function φ_0 is the only eigenfunction corresponding to the eigenvalue $+1$, and the system is ergodic.

Note that λ_1 and φ_1 are special, in that all other eigenvalues and eigenfunctions may be determined from these, since $\lambda_n = (\lambda_1)^n$ and $\varphi_n(x) = \varphi_1(x)^n$. However, because the eigenvalues are dense on the unit circle, there are eigenvalues arbitrarily close to λ_1, with eigenfunctions that are arbitrarily highly oscillatory. How could we distinguish the "primitive" eigenvalue λ_1 and its corresponding eigenfunction from the others, say, in a computer program? One way, suggested by Giannakis (3), is to normalize the eigenfunctions so that $\|\varphi_n\| = 1$ and then order them by their Dirichlet energy, which is given by

$$\text{Energy}(\varphi) = \|\nabla\varphi\|^2.$$

Thus, eigenfunctions that are more oscillatory will have higher Dirichlet energy. In our example, $\text{Energy}(\varphi_n) = (2\pi n)^2$, so the primitive eigenfunctions ($n = \pm 1$) are the ones with the least Dirichlet energy (other than the constant function, which has zero Dirichlet energy). The dense set of

[4] A measure-preserving system is ergodic if the only functions f that satisfy $Uf = f$ are constant almost everywhere.

eigenvalues still poses a computational challenge, and later sections present ways of regularizing the problem so that the eigenvalues of interest may be computed.

2.2. Example with Continuous Spectrum: Doubling Map

Next, consider the same state space $M = [0, 1)$, now with dynamics given by

$$Tx = 2x \pmod 1.$$

Although this map expands distances between points, Lebesgue measure is still preserved, since the preimage of any interval consists of two intervals, each half the length of the original interval [recall that the definition of measure preserving is that $\mu(A) = \mu(T^{-1}A)$].

This simple-looking system has surprisingly complicated dynamics. These dynamics can be understood by representing a point $x \in [0, 1)$ by its binary expansion, and noting that T acts to shift the decimal point (or binary point) to the right and throw out the whole-number portion; for instance,

$$0.100111 \mapsto 0.00111.$$

With this observation, it is straightforward to see that the system is chaotic in a deep sense. For instance, there are an infinite number of periodic orbits, all of which are unstable (these correspond to rational numbers, whose binary expansions are periodic); there are orbits of all periods; and there is a dense orbit.

Let us see what the Koopman operator U tells us about this system. Consider the function $f(x) = \exp(2\pi ix)$, and define the subspace S to be the span of $\{f, Uf, U^2f, \ldots\}$. Since $U^nf(x) = \exp(2\pi i \cdot 2^n x)$, the functions U^nf are mutually orthogonal, so the subspace S is infinite dimensional. On this subspace, the Koopman operator acts simply as a right-shift operator: If $g \in S$ has the form $g_0f + g_1(Uf) + g_2(U^2f) + \cdots$, then Ug has the form $0 \cdot f + g_0(Uf) + g_1(U^2f) + \cdots$, so U may be viewed as mapping the sequence $(g_0, g_1, g_2, \ldots)$ to the sequence $(0, g_0, g_1, g_2, \ldots)$. It is straightforward to show that the right-shift operator has no eigenvalues. In fact, even on the whole space $\mathcal{F}$, the Koopman operator U has only one eigenfunction: the constant function, corresponding to eigenvalue 1. The spectrum is now the unit disk, but all points on the unit circle besides $+1$ are in the continuous spectrum, and all points inside the unit disk are in the residual spectrum[5] (4) (see the sidebar titled The Continuous Spectrum).

In fact, a result of ergodic theory is that the Koopman operator has no eigenfunctions other than the constant function if and only if the system has a weak mixing property (10), a form of chaotic behavior that means that any subset of positive measure gets mixed uniformly in the phase space, in a time-averaged sense. Any system that is weakly mixing is also ergodic. Thus, the spectrum of the Koopman operator gives us information about this type of chaotic behavior.

There are several important takeaways from this example: First, the Koopman operator may have no eigenfunctions (besides the constant function), and second, chaotic systems that are weakly mixing have no eigenfunctions besides the constant function. For such chaotic systems, it is therefore not possible to define a coordinate as in Equation 2 such that the evolution is linear. However, Koopman-oriented methods may still be used for short-term prediction of these systems, as we shall see.

[5]If λ is not an eigenvalue and the range of $U - \lambda I$ is dense in $\mathcal{F}$ but not all of $\mathcal{F}$, then λ is in the continuous spectrum of U. If λ is not an eigenvalue and the range of $U - \lambda I$ is not dense in $\mathcal{F}$, then λ is in the residual spectrum of U.

THE CONTINUOUS SPECTRUM

An unfortunate misconception that has crept into the recent literature in this area is that the point spectrum consists of isolated points, and the continuous spectrum consists of a "continuum of eigenvalues." This is not the case: Eigenvalues do not belong to the continuous spectrum (see the definition given earlier for the term point spectrum, and footnote 5 for the definition of continuous spectrum). Furthermore, if U is an isometry and the Hilbert space $\mathcal{F}$ is separable, then it is not possible to have a "continuum of eigenvalues," since eigenfunctions corresponding to distinct eigenvalues are orthogonal, and there can be at most countably many mutually orthogonal functions.

It is important to note that the spectrum depends on the function space being considered. For instance, consider the dynamics of a simple pendulum, which may be written in action–angle coordinates as

$$\dot{\theta} = J, \qquad \dot{J} = 0,$$

where the angle θ is on the circle and the action J is in an interval $[a, b]$. Observe that the frequency of oscillation depends on J, which is one of the state variables. If the measure μ is the usual Lebesgue measure, then this system has a continuous spectrum, and its only eigenvalue is 1, as shown by Mezić (5). However, this system is not weakly mixing, and it is not even ergodic: Any function that is independent of θ is an eigenfunction with eigenvalue 1 (intuitively, it is clear that trajectories do not explore the whole phase space, since J is constant along a trajectory).

However, if the measure μ is taken to be the one-dimensional Lebesgue measure, confined to a particular value J_0 (zero for other values of J), then this system is a continuous-time version of that considered in Section 2.1 and is ergodic, with pure point spectrum. This approach is, in fact, the usual one taken in ergodic theory: One takes the space M to be a constant-energy surface in the larger phase space (4, sec. II.5). This point of view is also consistent with numerical methods such as those described by Lusch et al. (6), who found a parameterized family of models, each of which has pure point spectrum.

The importance of the continuous spectrum and its connection with weakly mixing systems was recognized immediately by Koopman & von Neumann (7). Recently, methods have been developed for short-time prediction of such systems (3, 8) and for calculating the continuous spectrum numerically (9).

2.3. Flows and the Koopman Generator

Now let us consider the continuous-time setting, in which time t lies in $\mathbb{R}$, the state space M is a manifold, and the dynamics of the state variable $x(t) \in M$ are governed by the ordinary differential equation

$$\frac{\mathrm{d}x}{\mathrm{d}t} = F(x), \tag{3.}$$

or by the corresponding flow map $\Phi^t : M \to M$:

$$x(t) = \Phi^t x(0).$$

As before, we assume that (M, μ) is a measure space and that the flow Φ^t is measure preserving. The Koopman operator is defined as before: We let $\mathcal{F} = L^2(M, \mu)$, and for any $f \in \mathcal{F}$, we define

$$U^t f(x) = f(\Phi^t x). \tag{4.}$$

Thus, for each time $t \in \mathbb{R}$, we obtain a corresponding Koopman operator $U^t : \mathcal{F} \to \mathcal{F}$, which is unitary (since Φ^t is invertible and measure preserving). Furthermore, U^t satisfies $U^{t+s} = U^t U^s$, which makes U^t into a one-parameter unitary group. Stone's theorem (4, sec. VIII.4) then tells us that U^t may be written in terms of its infinitesimal generator V, defined by

$$Vf = \lim_{t \to 0} \frac{1}{t}(U^t f - f). \tag{5.}$$

The operator V is skew symmetric (i.e., $V^* = -V$), its domain $D(V)$ is dense in $\mathcal{F}$, and it satisfies $U^t = e^{tV}$, for a suitable definition of the exponential map. For any $f \in D(V)$, we have

$$Vf(x) = \lim_{t \to 0} \frac{1}{t} \big(f(\Phi^t x) - f(x) \big) = \nabla f(x) \cdot F(x) = (F \cdot \nabla) f(x), \qquad 6.$$

so Vf is the directional derivative of f along the vector field F. One of the properties that makes the generator V especially useful is that, unlike the operator U^t, V satisfies the product rule: For $f, g \in D(V)$,

$$V(fg) = V(f)g + fV(g).$$

Note that U^t and V have the same eigenfunctions, since $V\varphi = \lambda\varphi \Leftrightarrow U^t\varphi = e^{\lambda t}\varphi$. As with the discrete-time case, if V has an eigenfunction φ, with eigenvalue λ, then one may define a coordinate or observable $z(t) = \varphi(x(t))$, which evolves according to

$$\frac{\mathrm{d}}{\mathrm{d}t} z(t) = \frac{\mathrm{d}}{\mathrm{d}t} \varphi(x(t)) = \nabla\varphi(x(t)) \cdot F(x(t)) = V\varphi(x(t)) = \lambda\varphi(x(t)) = \lambda z(t).$$

Thus, the coordinate z is decoupled from the other coordinates and evolves linearly in time.

2.4. Stochastic Systems

Many of the ideas discussed above for deterministic, ergodic systems may be applied to stochastic systems as well. Consider a random variable X_t, parameterized by time $t \geq 0$, that has the property that, given X_s with $s < t$, X_t is independent of X_τ for all $\tau < s$. Such a random variable is called a Markov process. If the joint probability of X_t and X_s depends only on the difference $t - s$, the Markov process is called time homogeneous.

Since the probability distribution of X_t is completely characterized by the expectation values of (measurable) functions $f(X_t)$, it is useful to consider the conditional expectation of $f(X_t)$ given the history $\{X_\tau\}_{\tau \leq s}$ for some $s \leq t$. In particular, if X_t is a time-homogeneous Markov process, then

$$\mathbb{E}\big[f(X_t) \mid \{X_\tau\}_{\tau \leq s} \big] = g(X_s)$$

is a new (measurable) complex-valued function g of the previous state X_s that depends only on the time difference $t - s$. This observation allows one to define the family of linear operators $\{U^t\}_{t \geq 0}$ that perform this mapping $f \mapsto g$ according to

$$(U^t f)(x) := \mathbb{E}\big[f(X_t) \mid X_0 = x \big]. \qquad 7.$$

In probability theory, this family $\{U^t\}_{t \geq 0}$ is called the Markov semigroup (11), while in dynamical systems, U^t is referred to as the (stochastic) Koopman operator (12–14).

For a deterministic dynamical system, the definition in Equation 7 agrees precisely with the definition given previously in Equation 4. On the other hand, for a stochastic dynamical system,

$$\mathrm{d}X_t = F(X_t)\mathrm{d}t + \mathrm{d}W_t,$$

subject to standard Brownian motion $\{W_t\}_{t \geq 0}$, the action of the Markov semigroup is determined by solving the Kolmogorov backward equation

$$\frac{\mathrm{d}}{\mathrm{d}t} (U^t f) = V (U^t f), \qquad U^0 f = f, \qquad 8.$$

where the infinitesimal generator V is given by the advection–diffusion operator

$$Vf = (F \cdot \nabla) f + \frac{1}{2} \nabla^2 f. \qquad 9.$$

In contrast to Equation 6 for a deterministic system, Equation 9 has a diffusive term $\nabla^2 f$ due to the presence of Brownian motion. This diffusion term also breaks the product rule that holds for the deterministic generator.

The stochastic Koopman (a.k.a. Markov) semigroup and its infinitesimal generator describe the evolution of functions on the state space, or observables. The adjoints of these operators govern the evolution of probability distributions over the state space. If the initial condition X_0 has probability density ρ_0, then X_t has density ρ_t satisfying the Fokker–Planck equation (a.k.a. the Kolmogorov forward equation),

$$\frac{\mathrm{d}}{\mathrm{d}t}\rho_t = V^*\rho_t = -\nabla \cdot (F\rho_t) + \frac{1}{2}\nabla^2\rho_t,$$

where V^* is the adjoint of the stochastic Koopman generator. The adjoint of the stochastic Koopman operator propagates probability densities forward in time and is called the Perron–Frobenius operator, or transfer operator.

2.5. Generalizations to Other Settings

In preceding sections, we have defined the Koopman operator for a measure-preserving dynamical system. This is the context in which the Koopman operator was originally considered, and it has played an important role in the field of ergodic theory. Ergodic theory studies the behavior of a system in the large-time limit, in which the state lives on an attractor. In this setting, there is a natural measure, and the theory as described above is well established.

Recently, there has been renewed interest in using the Koopman operator to describe the transient behavior of systems. This point of view is particularly of interest for control, in which one might want to use an input to change the transient behavior or stabilize a particular steady state. In this context, the theory as described above is not as suitable, since there is no longer a natural invariant measure, and the flow is typically not measure preserving. The introduction of a control input adds an additional wrinkle, as it is not immediately clear how to introduce an input into the formalism just presented. We will discuss recent developments in these areas in Section 4.

In this more general context, one can still choose a measure μ and define a Koopman operator on $L^2(\mu)$ as before (namely, by Equation 1 in discrete time or by Equation 4 or 5 in continuous time), although now this operator is not an isometry, since the system is not measure preserving. One also needs to be careful since U may be unbounded, and its domain may not include all functions in $L^2(\mu)$. In the next section, we shall see an example of how the Koopman operator can be useful for such systems.

2.6. Invariant Subspaces and Global Linearization

If the Koopman operator has enough eigenfunctions, it may be possible to find a nonlinear change of coordinates in which the dynamics are linear, at least within a particular region of state space. This point of view is particularly attractive for analysis of systems with transients, or for systems with a control input, since linear systems are easier to work with than nonlinear systems. In this section, we explain this idea and its close connection with the concept of invariant subspaces.

Assume we have a discrete-time system for which the state evolves according to $x(t+1) = Tx(t)$ and the Koopman operator is defined on a function space $\mathcal{F}$ as in Equation 1. Here, we do not restrict ourselves to measure-preserving systems, so U may not be an isometry. Consider a subspace S of $\mathcal{F}$ spanned by linearly independent functions $\{f_1, \ldots, f_n\}$. We say this subspace is invariant if $Uf \in S$ whenever $f \in S$.

If S is an invariant subspace, then this means that for any $j = 1, \dots, n$, we may write

$$Uf_j(x) = f_j(Tx) = \sum_{i=1}^{n} a_{ij} f_i(x), \qquad 10.$$

for some constants a_{ij}, which form the matrix representation of U with respect to the basis $\{f_j\}_{j=1}^n$. Let us call this matrix $\mathbf{U}$.

A few remarks are in order. First, if $\mathbf{v} = (v_1, \dots, v_n)$ is an eigenvector of $\mathbf{U}$ with eigenvalue λ, then the function $\varphi = \sum_{j=1}^n v_j f_j$ is an eigenfunction of U with eigenvalue λ, since

$$U\varphi = \sum_{j=1}^{n} v_j U f_j = \sum_{i,j=1}^{n} a_{ij} v_j f_i = \sum_{i=1}^{n} \lambda v_i f_i = \lambda \varphi.$$

Thus, if we can find an invariant subspace S, then we can easily find eigenvalues and (possibly generalized) eigenfunctions of U simply by solving an $n \times n$ eigenvalue problem for the matrix $\mathbf{U}$. Another observation is that, if the system is weakly mixing (so that U has no eigenfunctions besides the constant function), then the only finite-dimensional invariant subspace is the one-dimensional space spanned by the constant function.

Next, observe that if we define coordinates $z_j = f_j(x)$, then Equation 10 implies that the evolution of these coordinates is linear:

$$z_j(t+1) = f_j(x(t+1)) = Uf_j(x(t)) = \sum_{i=1}^{n} a_{ij} f_i(x(t)) = \sum_{i=1}^{n} a_{ij} z_i(t).$$

Furthermore, if the map $x \mapsto (f_1(x), \dots, f_n(x))$ is injective, then we may recover x from $(z_1, \dots, z_n)$, so we have determined a change of coordinates in which the dynamics are linear.

Thus, Koopman eigenfunctions can determine coordinates in which a system evolves linearly, and these coordinates may be viewed as a global linearization. Unfortunately, it is not always possible to determine such coordinates; for instance, such coordinates never exist for weakly mixing systems. In some special cases, however, it is possible to find such coordinates. For instance, Lan & Mezić (15) showed that for nonlinear systems consisting of a single globally attracting equilibrium point, it is always possible to find such coordinates. This result may be viewed as a global version of the Hartman–Grobman theorem, which states that in a neighborhood of a hyperbolic fixed point, there exists a nonlinear change of coordinates in which the dynamics are linear. Similar ideas have been developed for the basins of more general types of attractors, including limit cycles and quasi-periodic tori (5). Furthermore, the stability of more general invariant subsets has been studied by Mauroy & Mezić (16) using the Koopman operator over the invariant subspace of continuous functions supported on their complement. These results provide close connections between Koopman eigenfunctions and classical Lyapunov theory. In particular, the zero level sets of Koopman eigenfunctions are invariant sets, and if the associated Koopman eigenvalues lie inside the unit circle (or in the left half-plane for the generator), then a Lyapunov function for the intersection of several such zero level sets can be found by summing the squared magnitudes of the corresponding eigenfunctions (16). In a similar way, the magnitudes of Koopman eigenfunctions have a monotone time evolution, and so their level sets can be intersected to find trapping regions.

Finally, we note that, if U has an eigenfunction φ, then its magnitude and phase may be viewed as action–angle coordinates for the system. For instance, suppose that $U\varphi = \lambda\varphi$ with $\lambda = re^{i\theta}$. Then the coordinate $\varphi(x)$ evolves according to $\varphi(Tx) = U\varphi(x) = re^{i\theta}\varphi(x)$, or

$$|\varphi(x(t+1))| = r|\varphi(x(t))|, \qquad \angle\varphi(x(t+1)) = \angle\varphi(x(t)) + \theta,$$

so $|\varphi|$ and $\angle\varphi$ play the roles of action and angle variables, respectively. For systems that are asymptotically periodic, level sets of $\angle\varphi$ determine isochrons, as used by Mauroy and colleagues (17, 18). If the system is measure preserving, then eigenvalues lie on the unit circle, so $r = 1$ and $|\varphi(x)|$ remains constant along trajectories.

3. APPROXIMATING THE KOOPMAN OPERATOR FROM DATA

In this section, we give an overview of some techniques that have been developed over the past two decades to approximate the Koopman operator given data sampled from a dynamical system. One of the challenges in such an approximation is that the Koopman operator is not compact, and as we have seen, it may not have any eigenvalues (besides 1). Numerical approximations will necessarily be finite dimensional and will thus always have eigenvalues. To obtain a convergent numerical method and interpret its results, it is thus usually necessary to first "compactify" the Koopman operator, and various approaches to this are possible, as we discuss below.

3.1. Projection onto a Subspace

Most approaches for approximating the Koopman operator involve projecting the infinite-dimensional operator onto a finite-dimensional subspace. Consider the setting of the previous section, in which the Koopman operator U acts on a Hilbert space $\mathcal{F}$, and suppose we have an orthonormal basis $\{\phi_1, \phi_2, \ldots\}$ for $\mathcal{F}$. Let S_N denote the N-dimensional subspace spanned by $\{\phi_1, \ldots, \phi_N\}$, and define the projection of U onto S_N by

$$U_N f = \sum_{n=1}^{N} \langle \phi_n, Uf \rangle \phi_n. \tag{11.}$$

(We adopt the convention that inner products are linear in the second argument and conjugate linear in the first.) This approximation is the Galerkin projection of U onto this subspace, and the projected operator U_N may be represented by an $N \times N$ matrix with entries $\langle \phi_m, U\phi_n \rangle$.

If it happens that an eigenfunction φ of U lies in the subspace S_N, then it is straightforward to verify that φ is also an eigenfunction of U_N. More generally, if the subspace S_N is invariant under U (that is, if $Uf \in S_N$ whenever $f \in S_N$), then $U_N f = Uf$ for any $f \in S_N$. In this case, all of the eigenvalues and eigenfunctions of U_N are also eigenvalues and eigenfunctions of U, as discussed in Section 2.6.

Unfortunately, we usually are not so fortunate as to know a subspace S_N that is invariant or contains an eigenfunction of U; in fact, this is usually what we are trying to find. In practice, the operator U_N is an approximation of U, and we may consider in what sense U_N converges to U as $N \to \infty$.

If U is bounded, as is always the case in the measure-preserving setting (since it is an isometry), the sequence U_N will always converge pointwise—that is, for any $f \in L^2(\mu)$, $U_N f \to Uf$ (where convergence is in the L^2 norm; this follows immediately from the Parseval identity). This pointwise convergence is sufficient for short-term prediction of the dynamics—for instance, as one might need for model predictive control (as we shall consider in Section 4). It is tempting to conclude that the spectrum of U_N converges to the spectrum of U, but unfortunately this is not the case. For instance, consider the example from Section 2.2, in which U acts as a right-shift operator. In this case, for any N, the eigenvalues of U_N are all zero, yet U does not have any eigenvalues (besides 1), and its continuous spectrum lies on the unit circle. Thus, pointwise convergence is not enough to ensure that the spectrum of U_N says anything at all about the spectrum of U.

In addition, even if U has pure point spectrum, recall from Section 2.1 that the eigenvalues typically form a countable dense subset of the unit circle. As a result, sparse eigenvalue solvers may have difficulty, and it may not be straightforward to distinguish the most meaningful "primitive" eigenvalue.

For these reasons, schemes to approximate the Koopman operator typically use some sort of regularization in order to ensure that the eigenvalues or eigenvectors of a finite-dimensional approximation correspond to those of the original operator U. For instance, if an operator U is compact (not just bounded), then the sequence U_N as defined above converges to U not just pointwise, but uniformly (i.e., $\sup_{\|f\|=1} \|U_N f - Uf\| \to 0$), and in this case, eigenvalues and eigenvectors of U_N do converge to those of U. However, approximating the Koopman operator by a compact operator is not so straightforward, since compact normal operators have pure point spectrum, while for many systems of interest the Koopman operator does not.

Some of the primary differences between the methods discussed in this section come down to two choices: the subspace S_N to project onto and the type of regularization used. In some of the methods, the regularization is implicit, and in others it is explicit.

3.2. Set-Oriented Methods

Historically, the first data-driven methods were developed by Dellnitz & Junge (19) to approximate the adjoint of the Koopman operator, called the Perron–Frobenius operator, or transfer operator. As mentioned in Section 2.4, while the Koopman operator describes the evolution of functions on the state space, via composition with the flow map, the Perron–Frobenius operator describes the evolution of measures (or densities), via pushforward. In the L^2 setting, the two approaches are equivalent. Dellnitz & Junge (19) used a set-oriented method known as Ulam's method, in which the state space is divided into a finite number of disjoint subsets, and the transition probabilities between subsets are estimated numerically. The resulting Markov matrix is shown to approximate a version of the transfer operator, in this case made compact by the addition of a small amount of diffusion. This method may be viewed as a Galerkin projection in which the (orthogonal) basis functions are indicator functions on the disjoint subsets.

This approach has shown great success, especially in identifying almost-invariant sets (20) and coherent sets (21, 22), and may be used to compute the spectrum and eigenvectors of both the transfer operator and the Koopman operator (23). It has also been used to determine low-dimensional deterministic models for stochastic systems (13). However, this approach is not suitable if the dimension of the state space is large (more than approximately three or four), since the number of subsets required grows exponentially in the dimension.

3.3. Extended Dynamic Mode Decomposition

Dynamic mode decomposition (DMD) is a method proposed by Schmid (24) to identify coherent structures and their corresponding frequencies directly from data, without requiring knowledge of the underlying equations of motion. Its connection with the Koopman operator was pointed out by Rowley et al. (25). Here, we describe the extended dynamic mode decomposition (EDMD) method of Williams et al. (26).

Let us consider the discrete-time setting of the previous section, in which the dynamics are given by a map $T : M \to M$, where (M, μ) is a measure space, and the Koopman operator U acts on functions in $\mathcal{F} = L^2(M, \mu)$ according to $Uf = f \circ T$. We assume μ is a probability measure, but the dynamics are not necessarily measure preserving.

We start with a collection of functions $\psi_1, \ldots, \psi_N \in \mathcal{F}$, which are called observables. These functions span a subspace S_N on which we will project the Koopman operator. The functions ψ_n

may not be orthonormal, so the matrix representation $\mathbf{U}$ with respect to this basis satisfies the equations

$$\mathbf{GU} = \mathbf{A}, \qquad [\mathbf{G}]_{mn} = \langle \psi_m, \psi_n \rangle, \qquad [\mathbf{A}]_{mn} = \langle \psi_m, U\psi_n \rangle. \tag{12.}$$

(Here, $\mathbf{G}$ is called the Gram matrix, and it is the identity if the ψ_n are orthonormal.) The least squares solution of this system is given by $\mathbf{U} = \mathbf{G}^{+}\mathbf{A}$, where $\mathbf{G}^{+}$ denotes the Moore–Penrose pseudoinverse.

In this data-driven method, we do not assume we know the map T explicitly, or that we can evaluate the Koopman operator U on the functions ψ_n; thus, the inner products in Equation 12 cannot be computed explicitly. Instead, we assume we have access to observations $\psi_n(x_l)$, for a set of states $x_0, \ldots, x_{L-1}$, as well as their images $\psi_n(Tx_l)$ after one step of the dynamics. We then replace the inner products in Equation 12 with an empirical inner product

$$\langle f, g \rangle_L = \frac{1}{L} \sum_{l=0}^{L-1} \overline{f(x_l)} g(x_l), \tag{13.}$$

and then one can evaluate the terms in Equation 12 from the given data. Under certain assumptions on the sample data $\{x_l\}$, the empirical inner product given by Equation 13 approaches the inner product in $L^2(\mu)$ as $L \to \infty$; for instance, this happens if the system is ergodic and the states x_l arise from a single trajectory (i.e., $x_l = T^l x_0$) or if the states x_l are independently sampled according to the probability measure μ. Thus, in either of these cases, EDMD converges to a Galerkin method (Section 3.1) as the number of samples goes to infinity (26).

In this method, there is an implicit regularization imposed by the choice of basis functions (observables) ψ_n. In addition, it is common to employ an additional regularization when solving Equation 12: Rather than use the full pseudoinverse $\mathbf{G}^{+}$, one first forms a low-rank approximation of $\mathbf{G}$ and then finds the inverse. This is usually done by taking the singular value decomposition of the $N \times L$ matrix with entries $\psi_n(x_l)$, and then retaining only the largest r singular values. This procedure is equivalent to performing principal component analysis (or proper orthogonal decomposition) on the observed data and retaining the first r principal components.

The effectiveness of this data-driven method depends critically on the choice of observables ψ_n. If the observables ψ_n are the components of the states, EDMD reduces to the standard DMD (24). But many other choices are possible. For instance, one may use nonlinear functions of these state coordinates, such as monomials, orthogonal polynomials, radial basis functions, or even indicator functions on subsets, as in Ulam's method described in Section 3.2. Another natural choice is to use time-delayed coordinates (27)—that is, to choose a function f and take $\psi_n = f \circ T^n$. One may also use an implicit basis determined by a kernel function (28), in which case the (possibly infinite-dimensional) space of observables is the corresponding reproducing kernel Hilbert space (see Section 3.5.2).

The approach described here may also be used to approximate the Perron–Frobenius operator (29, 30) or the generators (31). While the spectrum of the EDMD approximation does not in general converge to the spectrum of the Koopman operator, a weak spectral convergence result is given by Korda & Mezić (32) in the special case that the observables $\{\psi_n\}$ are orthonormal. There are several other flavors of EDMD—for instance, to reduce the bias introduced by noisy measurements (33) or to select a small number of modes that describe the dynamics well (34).

An advantage of the EDMD approach is that it is computationally tractable even when the state dimension is large and when one has limited data (for instance, observations from a single trajectory). A challenge with this method is that a suitable choice of observables $\{\psi_n\}$ is often not clear. Eigenfunctions of U are often not approximated well by smooth functions, and one needs

a large number of basis functions; on the other hand, if N is large in comparison with L, then overfitting is a problem.

3.4. Neural Networks

One of the drawbacks of the approach described in the previous section is that one must decide a priori on a set of observables on which to project, and a suitable choice is not always clear. An alternative is to train a neural network to learn suitable observables from a given data set.

This idea has led to approximation techniques for the Koopman operator involving learned dictionaries (35) or deep learning autoencoders (36) suitably adapted for this task. The closely related approaches of References 6 and 37–42 utilize an autoencoder neural network together with recurrent linear dynamics in the latent space (e.g., see the learning architecture in Reference 41). By simultaneously training the weights defining the encoder, decoder, and evolution matrix on pairs or longer sequences of snapshots, these techniques are able to find a small set of observables that have (nearly) linear evolution in time and reconstruct the full state through a decoder neural network. The encoder provides a set of observables over which the transpose of the evolution matrix is an approximation of the Koopman operator.

Recurrent autoencoders are the only Koopman-oriented model identification technique where the observables are optimized simultaneously to meet the two criteria of informativeness (reconstructability) and Koopman invariance (linear evolution). This allows them to achieve superior performance over EDMD on several examples, including modeling the glycolysis pathway and power systems (40), vortex shedding in the wake of a cylinder (39, 41), and even making finite-horizon predictions of chaotic dynamical systems, including the Lorenz-63 model (37) and the Kuramoto–Sivashinsky equation (41).

Recurrent autoencoders also present a highly flexible learning architecture in which it would be essentially trivial to incorporate actuation. Later on, in Section 4 we will see that the evolution matrix is parameterized by the input, and this dependence could easily be learned from data. In addition, there is no reason that the evolution of the observables must be linear in this framework, and allowing for nonlinear evolution could be useful for systems that do not admit finite-dimensional Koopman-invariant subspaces, such as weakly mixing systems. Along these lines, Champion et al. (43) used a sparsity-promoting ℓ^1 penalty to select the terms governing the nonlinear dynamics of encoded observables from a dictionary. Although that approach was limited by the need for time derivatives of the state, we think that nonlinear evolution of the observables could be easily incorporated into existing recurrent autoencoder architectures using the "neural ODE" framework developed by Chen et al. (44).

One drawback of the neural network–based approach is that the optimization problem over all parameters in the encoder, decoder, and evolution matrix is nonconvex and high dimensional, so gradient descent may converge to a solution that is only locally optimal. In addition, one must manually tune the various hyperparameters, including the number and widths of layers in the encoder and decoder neural networks and the learning rate for gradient descent. In our own experience, however, the locally optimal solution one finds by training a recurrent autoencoder with carefully chosen hyperparameters is good enough to make superior predictions over short time horizons when compared with EDMD, as well as to learn the correct state-space geometry of the level sets of Koopman eigenfunctions (41).

3.5. Generator-Based Approaches for Ergodic Systems

In this section, we describe a family of methods developed specifically for ergodic systems. These methods overcome many of the drawbacks of the approaches mentioned previously, and they show

great promise, having performed exceptionally well on examples ranging from low-dimensional ordinary differential equations (3, 8, 45–47) to turbulent fluid flows (48).

Recall that one of the challenges of most Galerkin methods (such as EDMD) is to determine a suitable subspace for projection. Smooth basis functions often do not work well, and one often has to use a large dictionary of basis functions, which leads to problems with overfitting.

In the methods considered in this section, one learns an orthonormal basis for $L^2(\mu)$ directly from observation data. One then projects a suitably regularized version of the Koopman generator onto these basis functions and finds the corresponding eigenvalues and eigenfunctions. These can then be used to produce forecasts of the observed variables, even for systems that are weakly mixing (for which the nonregularized Koopman operator has no eigenfunctions).

Here, we discuss two variants of these methods, one based on manifold learning (3) and the other based on reproducing kernel Hilbert spaces (8). In both cases, we consider a continuous-time ergodic system as described in Section 2.3, with the following assumptions:

- The flow Φ^t preserves the measure μ and is ergodic.
- We are given data consisting of vector-valued measurements $\mathbf{f}(x_0), \dots, \mathbf{f}(x_{L-1})$ from a single time series $x_l = \Phi^{l\Delta t} x_0$.
- The time series is long enough to explore the attractor sufficiently well.
- The time step Δt is small enough that we can approximate the underlying vector field from adjacent samples.

3.5.1. Manifold learning and regularization by diffusion. In this approach, one determines a data-driven basis for $L^2(\mu)$ using manifold learning techniques, specifically the diffusion maps algorithm of Coifman & Lafon (49). The idea of this approach is to define a Laplace–Beltrami operator that describes a diffusion process on the sample points; then eigenfunctions of this operator form a basis for $L^2(\mu)$. In order to do this, we start with a kernel function—for instance, of the form

$$k(x_j, x_k) = \exp\left(-\frac{\|\mathbf{f}(x_j) - \mathbf{f}(x_k)\|^2}{\sigma^2}\right), \qquad 14.$$

where σ is a parameter describing the width of the kernel. Giannakis and colleagues (3, 46, 48) used a variable-bandwidth kernel introduced by Berry & Harlim (50), in which the width σ is a function of the points x_j, x_k, and can thus account for regions where the density of sample points varies.

We then construct an $L \times L$ affinity matrix $\mathbf{K}$ with entries $k(x_j, x_k)$. This matrix is normalized so that it may be viewed as a transition matrix of a Markov chain, and if the sample points arise from an ergodic system with invariant measure μ, then the eigenvectors of this matrix approximate an orthonormal basis of $L^2(\mu)$ (see 49, appendix A). Moreover, one can also determine weights $w_0, \dots, w_{L-1}$ such that the inner product in $L^2(\mu)$ may be approximated by

$$\langle f, g \rangle_L = \sum_{l=0}^{L-1} w_l \overline{f(x_l)} g(x_l).$$

With this data-driven basis in hand, one considers a suitably regularized version of the Koopman generator V (see Section 2.3) to project onto this basis. Regularization is a crucial step here, because the eigenvalues of V are usually dense on the imaginary axis,[6] which presents a challenge for sparse eigenvalue solvers and hinders our ability to find the most physically relevant eigenvalues.

[6]If λ_1 and λ_2 are eigenvalues of V, then $m\lambda_1 + n\lambda_2$ is also an eigenvalue for any integers m, n (thanks to the product rule). Hence, if any two eigenvalues of V are not rationally related, the eigenvalues will be dense on the imaginary axis.

Giannakis (3) achieved this regularization by adding a small amount of diffusion, defining the operator

$$\mathcal{L} = V + \alpha\Delta,$$

where $\alpha > 0$ is a parameter. The diffusion operator Δ is carefully constructed to commute with V, so that $\mathcal{L}$ and V have the same eigenvectors; eigenvalues of V are then the imaginary parts of the eigenvalues of $\mathcal{L}$.

Markov operator: an operator P that is positivity preserving, where $Pf = f$ if f is constant, and where $\int_M Pf \, d\mu = \int_M f \, d\mu$

As in the example in Section 2.1, we are interested in the smoothest (least oscillatory) eigenfunctions (e.g., as measured by Dirichlet energy), and the additional diffusion serves to damp out the more oscillatory eigenfunctions. A drawback of this regularization is that, unlike V, the regularized operator $\mathcal{L}$ is no longer skew symmetric. The next section describes a different type of regularization that does not have this drawback.

3.5.2. Reproducing kernel Hilbert spaces. A particularly elegant variant of the above approach formulates the problem using a kernel function and its corresponding reproducing kernel Hilbert space (8, 46, 47). A reproducing kernel Hilbert space is a Hilbert space $\mathcal{H}$ of complex-valued functions on M such that pointwise evaluation is a continuous linear functional. Thus, $\mathcal{H}$ has the property that two functions that are close in norm (i.e., with $\|f - g\|$ small) must also be close pointwise [i.e., with $|f(x) - g(x)|$ small for any $x \in M$]. Such spaces are especially useful when working with sampled data, since one wants to evaluate functions at given data points. In this sense, it is more natural to work in a reproducing kernel Hilbert space $\mathcal{H}$ than in $L^2(\mu)$, since pointwise evaluation in $L^2(\mu)$ may not even be well defined [strictly speaking, elements of $L^2(\mu)$ are not functions but rather are equivalence classes of functions, where two functions are equivalent if they differ only on a set of measure zero].

Because pointwise evaluation is a continuous linear functional on $\mathcal{H}$, the Riesz representation theorem guarantees the existence of a unique function $k : M \times M \to \mathbb{C}$, called the reproducing kernel, such that for any $f \in \mathcal{H}$, pointwise evaluation is given by

$$f(x) = \langle k(x, \cdot), f \rangle.$$

Conversely, the Moore–Aronszajn theorem (51) states that a given symmetric, positive-semidefinite kernel k gives rise to a unique reproducing kernel Hilbert space $\mathcal{H}$. The Gaussian kernel in Equation 14 is an example of a symmetric, positive-semidefinite kernel.

Now, suppose we have a measure μ and that our kernel k is square integrable with respect to μ. Then we can define an operator $K : L^2(\mu) \to \mathcal{H}$ by

$$Kf(x) = \int_M k(x, y) f(y) \, d\mu(y).$$

The kernel k is called a Markov kernel if the integral operator K is a Markov operator. The adjoint operator $K^* : \mathcal{H} \to L^2(\mu)$ is the inclusion map, which maps each function in $\mathcal{H}$ into its equivalence class in $L^2(\mu)$. Observe that K^*K is a Hilbert–Schmidt operator on $L^2(\mu)$ and hence is compact. Singular value decomposition of K gives an orthonormal basis $\{\phi_j\}_{j=1}^{\infty}$ for $L^2(\mu)$ and an orthonormal basis $\{\psi_j\}_{j=1}^{\infty}$ for $\mathcal{H}$, as well as values $\sigma_j > 0$ such that

$$K\phi_j = \sigma_j \psi_j, \qquad K^*\psi_j = \sigma_j \phi_j,$$

and K may be written

$$Kf = \sum_{j=1}^{\infty} \sigma_j \langle \phi_j, f \rangle \psi_j.$$

One of the important ideas of Das & Giannakis (47) was to use ϕ_j as basis functions for the space $L^2(\mu)$. In this approach, the kernel function is the same variable-bandwidth Gaussian kernel described in Section 3.5.1, suitably normalized so that it is Markov. The eigenfunctions ϕ_j of K^*K play the role of the eigenfunctions of the Laplace–Beltrami operator in Section 3.5.1.

Furthermore, Das et al. (8) used an elegant and effective regularization for V. In particular, while V is an operator on $L^2(\mu)$, they considered an operator on $\mathcal{H}$ defined by $W = KVK^*$. Like V, the operator W is skew symmetric, but while V is unbounded, W is compact (thanks to the compactness of K). Therefore, its spectrum consists entirely of eigenvalues and lies purely on the imaginary axis; furthermore, finite-dimensional approximations to W will converge uniformly, not just pointwise.

Das et al. (8) also introduced a generalization of the Dirichlet energy in the setting of a reproducing kernel Hilbert space. The Nyström extension operator $\mathcal{N} : D(\mathcal{N}) \to \mathcal{H}$ acts on a subspace $D(\mathcal{N})$ of $L^2(\mu)$ and in our setting is defined by

$$\mathcal{N}f = \sum_{j=1}^{\infty} \sigma_j^{-1} \langle \phi_j, f \rangle \psi_j.$$

The corresponding norm $\|f\|_{\mathcal{N}}^2 = \langle \mathcal{N}f, \mathcal{N}f \rangle_{\mathcal{H}}$ plays the role of the Dirichlet energy in the previous approach: A function with more energy in the higher modes (eigenfunctions corresponding to smaller singular values) will be larger in the $\|\cdot\|_{\mathcal{N}}$ norm.

Perhaps the most remarkable feature of the approach of Das et al. (8) is that one can obtain spectral convergence, even for weakly mixing systems. Starting with a particular Markov kernel k, one defines a family of Markov kernels k_τ, parameterized by $\tau > 0$ (which intuitively represents the time of diffusion of a Markov kernel). This family of kernels induces a family of spaces $\mathcal{H}_\tau$ and operators $K_\tau : L^2(\mu) \to \mathcal{H}_\tau$ and is carefully chosen such that the bases $\{\varphi_j\}$ and $\{\psi_j\}$ arising from singular value decomposition of the original kernel k are the same as for k_τ (apart from normalization). From the Koopman generator V, one then introduces a family of compact operators $W_\tau = K_\tau V K_\tau^*$. Because V and W_τ are both skew symmetric, they may be decomposed in terms of projection-valued measures E and E_τ, such that

$$V = \int_{\mathbb{R}} i\omega \, \mathrm{d}E(\omega), \qquad W_\tau = \int_{\mathbb{R}} i\omega \, \mathrm{d}E_\tau(\omega),$$

and Das & Giannakis (47) showed that E_τ converges[7] to E as $\tau \to 0$. This remarkable result implies that if V has eigenfunctions, eigenfunctions of W_τ will converge to these as $\tau \to 0$. But it applies even if the system is weakly mixing or has a mixed spectrum; furthermore, eigenfunctions of W_τ will always provide an orthonormal basis for $\mathcal{H}_\tau$ (since W_τ is compact).

Figure 1 shows an example from Das et al. (8) of this approach applied to the Rössler system, a system of three ordinary differential equations that has chaotic behavior similar to that of the Lorenz-63 model. **Figure 1*a*** shows imaginary parts of the eigenvalues $i\omega$ of W_τ, colored by the Dirichlet energy. Observe that for integer frequencies $\omega = 1, 2, 3, \ldots$, the Dirichlet energy remains small as τ decreases, while for other frequencies, the energy grows as τ decreases. The eigenfunction corresponding to $\omega = 1$ (**Figure 1*b***) shows a dependence on the angle about the vertical axis, and indeed the dynamics of the Rössler system have a regular angular motion about this axis. The motion in the radial direction is more irregular, as reflected in the eigenfunction corresponding to **Figure 1*c***. Even though this system has chaotic dynamics, these eigenfunctions (along with others) were used by Das et al. (8) to provide data-driven forecasts that are accurate over a surprisingly long time interval.

[7] Strictly speaking, this convergence is up to a unitary transformation, since E_τ and E act on different spaces.

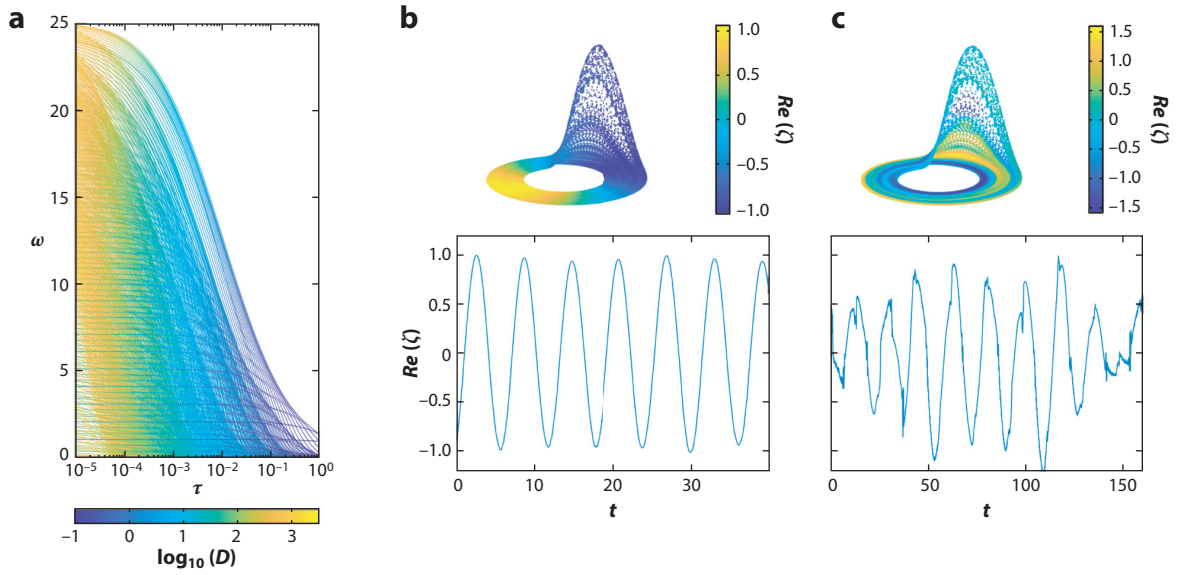

Figure 1

(*a*) Eigenfrequencies ω_j of the regularized Koopman generator W_τ, as a function of τ, for the Rössler system, colored by the Dirichlet energy D. (*b*) Real part of the eigenfunction ζ corresponding to $\omega = 1.03$ ($D = 0.608$) (*top*) and its value along a trajectory (*bottom*). (*c*) Real part of the eigenfunction corresponding to $\omega = 0.355$ ($D = 75.3$) (*top*) and its value along a trajectory (*bottom*). Figure adapted with permission from Reference 8.

4. CONTROL AND ESTIMATION USING KOOPMAN-ORIENTED MODELS

In this section, we discuss current research directions that aim to extend the Koopman framework to systems with actuation. This is an attractive perspective for control since the evolution of observables naturally encodes global information about the dynamics and, as we discussed near the end of Section 2.6, is closely related to classical Lyapunov stability theory. To study systems with actuation and develop successful control strategies, it is necessary to extend the classical understanding of Koopman operators developed for measure-preserving systems into the transient non-measure-preserving regime. In this section, we discuss recent approaches toward incorporating actuation into the Koopman framework as well as how to identify corresponding finite-dimensional models. While the powerful approximation tools developed in the measure-preserving setting will not be available, straightforward modifications of EDMD will yield pointwise convergent models that are sufficient to make the short-time predictions required for control and estimation applications. Finally, we discuss some of the successful control-oriented applications of these ideas.

4.1. Introducing Actuation into the Koopman Framework

So far, we have studied autonomous dynamical systems and time-homogeneous Markov processes, focusing primarily on the measure-preserving setting. Yet when actuation is introduced, the system becomes nonautonomous (nonhomogeneous) and may not be measure preserving. Hence, it is necessary to generalize the definitions of the Koopman operator and generator as well as their relationship via the exponential map in a way that allows us to study systems with actuation in this framework.

Williams et al. (52) made this generalization in a straightforward way by observing that when the input is held constant over a time interval of length t, the system is autonomous (homogeneous) over this interval. Therefore, the time-t Koopman operators U_u^t are parameterized by the input u and defined in the usual way according to Equation 4 for a deterministic system or Equation 7 for a stochastic system.

To define the Koopman generator in this setting, one must be a little careful; because the actuated Koopman operators U_u^t may not be unitary when the actuated system is not measure preserving, the methods used in Section 2.3 (e.g., Stone's theorem) do not apply. However, analogous results may be obtained using the notion of strongly continuous semigroups (53).[8] In particular, for a deterministic system $\dot{x} = F(x, u)$ and a stochastic system $\mathrm{d}x = F(x, u)\,\mathrm{d}t + \mathrm{d}W_t$, the Koopman generator V_u is defined by

$$V_u f = (F(\cdot, u) \cdot \nabla) f \qquad \text{and} \qquad V_u f = (F(\cdot, u) \cdot \nabla) f + \frac{1}{2}\nabla^2 f, \tag{15.}$$

respectively. These are directly analogous to Equations 6 and 9, respectively. As in the measure-preserving case, the domain of V_u is dense in $\mathcal{F}$, and the corresponding Koopman operator is given by a suitably defined exponential map, $U_u^t = \exp(V_u t)$ (see 53, chap. 1, theorem 8.3).

For control-oriented applications, a common approach is to build a finite-dimensional model of the Koopman operator or generator on a dictionary of observables. One key takeaway is that if the underlying dynamical system has simple (e.g., control-affine) dependence on the input, then so does the Koopman generator, making it an especially useful tool for building simplified models of the dynamics. The same cannot be said for the Koopman operator since the exponential map has complicated dependence on sums of noncommuting operators, often making the appropriate model of the input dependence unclear. The bilinear models arising from control-affine dynamics as well as the special case in which the dynamics of observables are linear and time invariant (LTI) are the most widely studied model types in the literature, and so we shall sketch what is known about them here.

4.1.1. Control-affine dynamics and bilinear Koopman generator models. As recognized by Surana (54), if a dynamical system is control affine, then its associated Koopman generator is also control affine—that is, with a slight generalization,

$$F(x, u) = F_0(x) + \sum_{k=1}^{K} \theta_k(u) F_k(x) \qquad \Rightarrow \qquad V_u = V_0 + \sum_{k=1}^{K} \theta_k(u) V_k, \tag{16.}$$

where $\theta_1, \ldots, \theta_K$ denote scalar-valued functions of the input u, and V_k refers to the Koopman generator associated with the component vector field F_k. Moreover, Mauroy & Goncalves (55) observed that the converse is also true: If $\boldsymbol{\psi} = (\psi_1, \ldots, \psi_d) : M \to \mathbb{C}^d$ is a vector of observables in the chosen function space $\mathcal{F}$ such that the derivative $\mathrm{D}\boldsymbol{\psi}(x)$ is injective for all $x \in M$, then the dynamics $F(x, u)$ in the form of Equation 16 can always be recovered from the formula

$$\mathrm{D}\boldsymbol{\psi}(x) F(x, u) = (V_0 \boldsymbol{\psi})(x) + \sum_{k=1}^{K} \theta_k(u) (V_k \boldsymbol{\psi})(x).$$

Let us focus on the control-affine setting, where the input u is a vector $(u_1, \ldots, u_K)$ and $\theta_k(u) = u_k$. If there is a dictionary $\boldsymbol{\psi} : M \to \mathbb{C}^d$ spanning an invariant subspace

[8] An operator semigroup $\{U^t\}_{t \geq 0}$ on a Banach space $\mathcal{F}$ is called strongly continuous if $U^t f \to f$ as $t \to 0^+$ for every $f \in \mathcal{F}$.

of the drift Koopman generator V_0, then one obtains the control-affine model

$$\frac{\mathrm{d}}{\mathrm{d}t}\mathbf{z} = \mathbf{V}_0^{\mathrm{T}}\mathbf{z} + \sum_{k=1}^{K} u_k \left(V_k \boldsymbol{\psi}\right)(x), \qquad \mathbf{z} := \boldsymbol{\psi}(x),$$

although components of $V_k\boldsymbol{\psi}$ may not lie in the span of $\{\psi_1, \ldots, \psi_d\}$. While such a model can provide significant dimensionality reduction, e.g., when $\{\psi_n\}$ are coordinates on an inertial manifold, the nonlinearity might still be quite complicated, perhaps even more complicated than the original governing equations. For such a case, Surana (54) reviewed a body of work showing that it is possible to design provably convergent observers for such systems when the observations $\mathbf{y} = \mathbf{g}(x)$ lie in the span of $\{\psi_1, \ldots, \psi_d\}$ and the nonlinearity $\mathrm{D}\boldsymbol{\psi}(x)F_k(x)$ has a sufficiently small Lipschitz constant.

As pointed out by Surana (54), Goswami & Paley (56), and Huang et al. (57), if $\{\psi_1, \ldots, \psi_d\}$ spans a subspace that is also invariant for each of the Koopman generators V_k, then the dynamics of these observables are described by a convenient bilinear model,

$$\frac{\mathrm{d}}{\mathrm{d}t}\mathbf{z} = \mathbf{V}_0^{\mathrm{T}}\mathbf{z} + \sum_{k=1}^{K} u_k \mathbf{V}_k^{\mathrm{T}}\mathbf{z}. \tag{17.}$$

In this case, Surana (54) pointed out that it becomes easier to design provably convergent observers, and conditions for nonlinear observability are derived based on the matrices $\mathbf{V}_0, \mathbf{V}_1, \ldots, \mathbf{V}_K$ and $\mathbf{C}$, where $\mathbf{y} = \mathbf{C}\mathbf{z}$ are the observations. From the control perspective, Goswami & Paley (56) derived conditions for the nonlinear controllability of Equation 17 and analyzed the reachable set using the Lie-algebraic approach of Brockett (58).

4.1.2. Linear time-invariant models for nonlinear observables. It is particularly useful if one can find observables $\mathbf{z} = \boldsymbol{\psi}(x)$ such that the dynamics of the original nonlinear system take the form of an LTI system:

$$\frac{\mathrm{d}}{\mathrm{d}t}\mathbf{z} = \mathbf{A}\mathbf{z} + \mathbf{B}u.$$

This class of systems has gained a lot of attention (39, 59–64) because all of the tools from linear control theory can be brought to bear. While it is too much to expect that a general nonlinear system may be represented as an LTI system, it is worth exploring the special cases when the system (or a useful approximation) may be written in this form. In general, if the observables $\boldsymbol{\psi}$ are sufficient to reconstruct the original vector field [i.e., $\mathrm{D}\boldsymbol{\psi}(x)$ is injective for all $x \in M$], then the transformed system is an LTI system if and only if the components of $\boldsymbol{\psi}$ span an invariant subspace of the Koopman generator associated with F_0, and in addition the underlying system is control affine, with

$$\dot{x} = F_0(x) + \sum_{k=1}^{K} u_k F_k(x), \qquad \text{where} \qquad F_k(x) \cdot \nabla\psi_i(x) = B_{i,k} = \text{constant} \quad \forall i, k.$$

In particular, $\mathbf{A} = \mathbf{V}_0^{\mathrm{T}}$ is given by the matrix approximation of the Koopman generator associated with the drift vector field in the basis $\boldsymbol{\psi}$.

The sidebar titled Linear Time-Invariant Models Are Delicate gives an example, adapted from Brunton et al. (65), showing that the assumptions required for a nonlinear system to be able to be transformed into LTI form are quite restrictive. In particular, the condition that all $F_k(x) \cdot \nabla\psi_i(x)$ are constant is difficult to achieve in practice. Nonetheless, these models encompass a strictly larger class than linear systems, possibly allowing them to achieve larger regions of validity when they are used for data-driven approximations.

LINEAR TIME-INVARIANT MODELS ARE DELICATE

Consider the following nonlinear actuated dynamical system, adapted from Brunton et al. (65):

$$\frac{\mathrm{d}}{\mathrm{d}t}\begin{bmatrix} x_1 \\ x_2 \end{bmatrix} = \begin{bmatrix} ax_1 \\ b(x_2 - x_1^3) \end{bmatrix} + u\begin{bmatrix} 0 \\ 1 \end{bmatrix} = F_0(x) + uF_1(x).$$

It is easy to check that the observables $\psi_1(x) = x_1$, $\psi_2(x) = x_2$, and $\psi_3(x) = x_1^3$ span a Koopman-invariant subspace for the drift F_0 and satisfy

$$F_1 \cdot \nabla\psi_1 = B_{1,1} = 0, \quad F_1 \cdot \nabla\psi_2 = B_{2,1} = 1, \quad F_1 \cdot \nabla\psi_3 = B_{3,1} = 0.$$

Therefore, the dynamics of these observables are described by an LTI system:

$$\frac{\mathrm{d}}{\mathrm{d}t}\begin{bmatrix} \psi_1 \\ \psi_2 \\ \psi_3 \end{bmatrix} = \begin{bmatrix} a & 0 & 0 \\ 0 & b & -b \\ 0 & 0 & 3a \end{bmatrix}\begin{bmatrix} \psi_1 \\ \psi_2 \\ \psi_3 \end{bmatrix} + \begin{bmatrix} 0 \\ 1 \\ 0 \end{bmatrix} u.$$

This example is not suitable for control, however, since the original system is uncontrollable. If the input is instead added to the $\dot{x}_1$ equation, so that the system is controllable [i.e., $F_1 = (1, 0)$ instead of $(0, 1)$], then we find that $F_1(x) \cdot \nabla\psi_3(x) = 3x_1^2$ is no longer constant. Therefore, the dynamics of the observables ψ are not LTI in this case. However, if one includes the observables 1 and x_1^2, then the dynamics are bilinear, as discussed in Section 4.1.1; in particular, we have

$$\frac{\mathrm{d}}{\mathrm{d}t}\begin{bmatrix} 1 \\ x_1 \\ x_2 \\ x_1^2 \\ x_1^3 \end{bmatrix} = \begin{bmatrix} 0 & 0 & 0 & 0 & 0 \\ 0 & a & 0 & 0 & 0 \\ 0 & 0 & b & 0 & -b \\ 0 & 0 & 0 & 2a & 0 \\ 0 & 0 & 0 & 0 & 3a \end{bmatrix}\begin{bmatrix} 1 \\ x_1 \\ x_2 \\ x_1^2 \\ x_1^3 \end{bmatrix} + u\begin{bmatrix} 0 & 0 & 0 & 0 & 0 \\ 1 & 0 & 0 & 0 & 0 \\ 0 & 0 & 0 & 0 & 0 \\ 0 & 2 & 0 & 0 & 0 \\ 0 & 0 & 0 & 3 & 0 \end{bmatrix}\begin{bmatrix} 1 \\ x_1 \\ x_2 \\ x_1^2 \\ x_1^3 \end{bmatrix}.$$

This example illustrates that the requirements that must hold in order for a nonlinear system to be written (exactly) in LTI form are quite restrictive. However, approximate models of this form can nevertheless be useful for controller synthesis and could provide sufficient accuracy for estimation and control over a larger region of state space than the standard approach of linearizing about a fixed point.

4.2. Approximation Techniques with Actuation

Most applications of the Koopman operator and generator to control and estimation problems rely on models of the dynamics built from finite-dimensional approximations of these operators. In this section, we discuss techniques for identifying finite-dimensional approximations of the Koopman operator and generator that include input parameterization. The main techniques used in the literature are Carleman linearization (66–68) and modified versions of EDMD (31, 52, 59, 60). Both techniques can be used to approximate the Koopman generator when the governing equations are known, while EDMD-based techniques can rely solely on snapshot data collected from the system.

4.2.1. Carleman linearization. Carleman linearization (66) is a technique by which analytic systems of nonlinear equations can be transformed into infinite-dimensional linear systems via Taylor series. Finite-dimensional models with explicit error bounds (69) can then be obtained by truncating the series. This technique has been used extensively to describe and compute analytic

flows of nonlinear differential equations (70, 71), including applications to control (67) and state estimation (68). While the technique has also been extended to study analytic partial differential equations using Lie series (72), we will focus on ordinary differential equations.

The main idea is to recognize that the Taylor series coefficients of an analytic function f are given by a linear map $Cf = (c_\alpha f)_{\alpha \in \mathbb{N}^n}$. More precisely, if we let our dictionary consist of monomials $\psi_\alpha(x) := (x - x_0)^\alpha$ for every multi-index $\alpha = (\alpha_1, \ldots, \alpha_n) \in \mathbb{N}^n$, then Taylor's theorem gives

$$f(x) = \sum_{\alpha \in \mathbb{N}^n} \psi_\alpha(x) c_\alpha f, \qquad \text{where} \qquad c_\alpha f := \frac{1}{\alpha!} \partial^\alpha f(x_0).$$

If the underlying dynamical system is analytic, then the Koopman generator maps analytic functions to analytic functions. Hence, the generator is described by the infinite "matrix" $[\mathbf{V}_u]_{\alpha,\beta} = c_\alpha V_u \psi_\beta$ acting on Taylor series coefficients, allowing the dynamics of analytic observables to be expressed as

$$V_u f = \sum_{\alpha \in \mathbb{N}^n} \psi_\alpha \left(\sum_{\beta \in \mathbb{N}^n} [\mathbf{V}_u]_{\alpha,\beta} \, c_\beta f \right).$$

In most applications of Carleman linearization, one is interested in predicting the evolution of the full state. In such a case, the dictionary can be built recursively, starting with the full state observable and adding monomials as they are needed to express $V_u \psi_\alpha$ as given by Equation 15 for the monomials ψ_α already in the dictionary. This idea was discussed by Brunton et al. (65) in order to study systems that admit finite-dimensional Koopman-invariant subspaces that contain the full state observable.

4.2.2. Modifications of extended dynamic mode decomposition. The EDMD technique discussed in Section 3.3 can be modified in a natural way to construct finite-dimensional approximations of the Koopman generator, as shown by Klus et al. (31) for both deterministic and stochastic systems. This approach is referred to as gEDMD. In particular, the only change is to the definition of the matrix $\mathbf{A}$, which is now parameterized by the input u and defined by

$$[\mathbf{A}_u]_{m,n} = \langle \psi_m, V_u \psi_n \rangle .$$

The action of the Koopman generator on the observable ψ_m can be found by using the governing equations explicitly or by using finite differences to approximate $\dot{x}$ from short time series and constructing $(V_u \psi_n)(x) = \dot{x} \cdot \nabla \psi_n(x)$. The finite-dimensional input-parameterized matrix approximation of the Koopman generator obtained by data-driven Galerkin projection into the span of $\{\psi_n\}$ is then given by $\mathbf{V}_u = \mathbf{G}^+ \mathbf{A}_u$, where $\mathbf{G}$ is the Gram matrix defined in Section 3.3.

Even if the governing equations are unknown, one does not always have to perform gEDMD at every input level u. If one knows that the dynamics are control affine, for instance, then one option is to expand the input in a basis $u = \sum_i u_i e_i$ and construct matrix approximations $\mathbf{V}_{e_i}$ for each of the generators V_{e_i} separately (each using the same dictionary $\{\psi_n\}$) using gEDMD. Using the control-affine property of the generator, the corresponding finite-dimensional matrix approximation for any actuation level u is then given by

$$\mathbf{V}_u = \mathbf{V}_0 + \sum_i u_i \left(\mathbf{V}_{e_i} - \mathbf{V}_0 \right),$$

as discussed by Peitz et al. (73).

When the governing equations are not known explicitly, we can postulate how the Koopman generator or operator depends on the input based on the discussion in Section 4.1 and search for a best-fit model to a collection of data as proposed by Williams et al. (52). Recent methods such as dynamic mode decomposition with control (DMDc) (59) and extended dynamic mode

decomposition with control (EDMDc) (60) are special cases of this idea where an LTI model of the form discussed in Section 4.1.2 is assumed. The data used to approximate the Koopman generator using this technique consist of states $\{x_l\}$, inputs $\{u_l\}$, and the resulting time derivatives $\{\dot{x}_l\}$ obtained from the governing equation or by finite differences. Recognizing that the matrix approximations given by EDMD or gEDMD solve a least squares problem, Williams et al. (52) computed each matrix $\mathbf{V}_k$ in a basis expansion $\mathbf{V}_u := \sum_{k=1}^{K} \theta_k(u)\mathbf{V}_k$ simultaneously by solving the least squares problem (stated for the generator)

$$\underset{\mathbf{V}_1,\ldots,\mathbf{V}_K}{\text{minimize}} \sum_{l=0}^{L-1} \left\| \left(V_{u_l}\boldsymbol{\psi}\right)(x_l) - \sum_{k=1}^{K} \theta_k(u_l)\mathbf{V}_k^{\mathrm{T}}\boldsymbol{\psi}(x_l) \right\|_2^2. \tag{18.}$$

where, as in Section 4.1.1, θ_k are predetermined functions of the input. The solution may be obtained by defining an empirical inner product between functions of the state and input according to

$$\langle f, g\rangle_L = \frac{1}{L}\sum_{l=0}^{L-1} \overline{f(x_l,u_l)}\, g(x_l,u_l).$$

With this definition and $\mathbf{W}$ denoting the matrix formed by vertically stacking $\mathbf{V}_1, \mathbf{V}_2, \ldots$, the normal equations for the least squares problem in Equation 18 become

$$\mathbf{GW} = \mathbf{A}, \qquad [\mathbf{G}]_{m,n} = \langle [\boldsymbol{\theta}\otimes\boldsymbol{\psi}]_m, [\boldsymbol{\theta}\otimes\boldsymbol{\psi}]_n\rangle_L, \qquad [\mathbf{A}]_{m,n} = \left\langle [\boldsymbol{\theta}\otimes\boldsymbol{\psi}]_m, \tilde{V}\psi_n \right\rangle_L,$$

where $\otimes$ denotes the Kronecker product, $\boldsymbol{\theta} = (\theta_1, \ldots, \theta_K)$, and $(\tilde{V}\psi_n)(x,u) = (V_u\psi_n)(x)$. A solution of the least squares problem is given by the familiar Moore–Penrose inverse $\mathbf{W} = \mathbf{G}^{+}\mathbf{A}$ and is the unique solution if there are enough data to make $\mathbf{G}$ full rank. In general, the data requirement scales with the number of basis functions θ_n times the number of dictionary functions ψ_n.

4.2.3. Dimension reduction of Koopman-oriented models. The accuracy of the EDMD-based techniques described in Section 4.2.2 increases with the number of dictionary functions and the amount of data. However, there is a corresponding growth in the dimension of the models that are obtained using these approaches. If we have obtained an accurate but high-dimensional Koopman-oriented model, it is reasonable to ask whether a smaller number of especially informative observables can be chosen. Some notable approaches along these lines include sparsity-promoting DMD (34), reducing overspecified systems via balanced truncation (41, 74), selecting approximate eigenfunctions based on an accuracy criterion (75), and optimizing the learning subspace via optimal mode decomposition (76).

Sparsity-promoting DMD and eigenfunction selection techniques approach the same problem of choosing a small collection of Koopman eigenfunctions from two different points of view. In sparsity-promoting DMD, sparse regression utilizing an ℓ^1 penalty is used to select a small collection of Koopman eigenfunctions that can be used, together with their known evolution, to reconstruct time histories obtained from a system. On the other hand, eigenfunction selection based on accuracy criteria is blind to the reconstruction and chooses approximate eigenfunctions obtained from data-driven methods according to whether they actually evolve as true eigenfunctions on a held-out set of evaluation data.

To apply these ideas to systems with a control input, it is conceivable that a technique like sparsity-promoting DMD could be used to select from the Koopman eigenfunctions associated with the drift Koopman operator U_0^t, a collection that can reconstruct data from the actuated system. Let $\mathbf{C}$ be a matrix of coefficients approximating the full state observable in the span of the drift Koopman eigenfunctions $\boldsymbol{\varphi}$ so that $x \approx \mathbf{C}\boldsymbol{\varphi}(x)$, and let $\mathbf{V}_u$ denote the input-parameterized

matrix approximation of the generator in this basis. Note that the coefficients $\mathbf{C}$ can be found by the same data-driven Galerkin method employed in EDMD (26) and are often referred to as approximate Koopman modes (25). Using the known matrices $\mathbf{C}$ and $\mathbf{V}_u$, we might try to reconstruct the evolution of snapshots

$$\Phi^t_{u_l} x_l \approx \mathbf{C} \exp(\mathbf{V}_{u_l} t)^{\mathrm{T}} \mathbf{z}_l$$

by optimizing over the vectors $\mathbf{z}_l$ subject to a sparsity-promoting ℓ^1 penalty on the rows of $\mathbf{Z} = [\mathbf{z}_1 \ \cdots \ \mathbf{z}_L]$. Since $\mathbf{z}_l$ is a surrogate for $\boldsymbol{\varphi}(x_l)$ in the above equation, this penalty should implicitly select an invariant subspace of the drift that is also nearly invariant when actuation is applied.

Koopman modes: coefficients used to expand an observable, usually the state, in a Koopman eigenfunction basis

4.3. Applying Models with Actuation for Control and Estimation

The techniques described above allow us to (perhaps approximately) transform a system of the form $\mathrm{d}x/\mathrm{d}t = F(x, u)$ into the form

$$\mathbf{z}(t + \Delta t) = \left(\mathbf{U}_u^{\Delta t}\right)^{\mathrm{T}} \mathbf{z}(t) \qquad \text{or} \qquad \frac{\mathrm{d}}{\mathrm{d}t}\mathbf{z} = (\mathbf{V}_u)^{\mathrm{T}}\, \mathbf{z}, \qquad \mathbf{z} := \boldsymbol{\psi}(x), \tag{19.}$$

with observations $\mathbf{y} = \mathbf{C}\mathbf{z}$. Why would we be interested in models of this form instead of the original state-space system? There are two main advantages to be gained from these representations.

The first advantage is increased efficiency for prediction and optimization. In particular, by using nonlinear observables $\boldsymbol{\psi}$, one might be able to predict the dynamics of quantities of interest with sufficient accuracy for the desired application at reduced computational cost. In particular, low-cost predictions are possible when the observables provide significant dimensionality reduction when compared with the full state dynamics. Recent work by Peitz and colleagues (73, 77) has leveraged this idea for model predictive control (MPC) of high-dimensional systems, including a viscous Burgers equation and simulated fluid flows. In Reference 77, the input takes one of a finite number of discrete values $\{u_k\}$ over finite time intervals, and the matrix approximations $\mathbf{U}_{u_k}^{\Delta t}$ of the underlying Koopman operators associated with each autonomous system are used to make predictions on a small enough dictionary of observables to enable efficient switched-system MPC for partial differential equations. The approach was later extended to continuously varying inputs for control-affine systems in Reference 73, where the bilinear structure of the associated model was leveraged together with the dimensionality reduction provided by the observables for efficient optimization of the control signal in the MPC framework.

The second advantage is that the special structure of the models can be exploited for controller and observer design. For instance, special forms of the models in Equation 19 can improve computational feasibility of controller/observer synthesis and can enlarge the region of validity of the resulting controllers/observers. The two special forms that have gained the most attention in the literature are bilinear models arising from control-affine systems (Section 4.1.1) and LTI models for the dynamics of nonlinear observables (Section 4.1.2).

Bilinear models were leveraged by Huang et al. (57, 78) for controller synthesis based on control Lyapunov functions found by solving a convex semidefinite optimization problem. In Reference 57, the goal was to stabilize one of the unstable fixed points of the chaotic Lorenz-63 system. The approach used an approximate bilinear model identified by EDMD with a dictionary $\boldsymbol{\psi}$ consisting of monomials up to degree three in the three state variables. While there is no nontrivial finite-dimensional Koopman-invariant subspace for this system due to the mixing property of the chaotic dynamics, the approximate bilinear model obtained by EDMD was accurate enough to synthesize an effective controller. The trajectories from five different initial conditions with and without feedback control are shown in **Figure 2**. As can be seen in the figure, the controller is effective for all of the initial conditions.

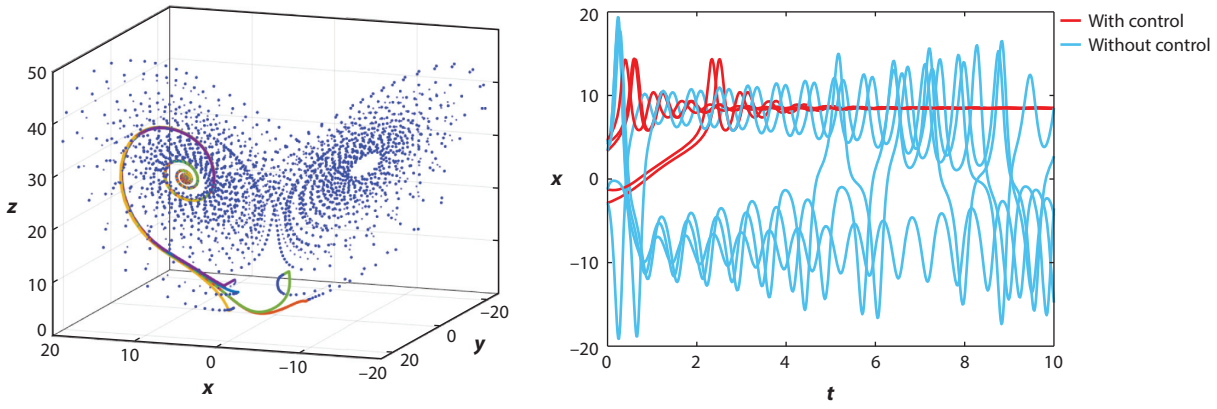

Figure 2

Examples of the use of a technique based on a control Lyapunov function to stabilize one of the fixed points of a chaotic Lorenz-63 system using an approximate bilinear model built from monomial observables up to degree three. Trajectories from five different initial conditions are shown, both with and without feedback control. Figure adapted with permission from Reference 57.

Korda & Mezić (60) leveraged the LTI dynamics of nonlinear observables to approximate MPC problems for nonlinear systems using convex quadratic programs that can be solved as efficiently as the analogous problems for linearized state-space models. These techniques were used by Korda et al. (61) to stabilize a nonlinear model of seven coupled power grids undergoing an instability due to a simulated power-line failure.

EDMD-based identification techniques (Section 4.2.2) can also increase the region of approximate validity for Koopman-oriented models—for instance, as compared with Carleman linearization (Section 4.2.1)—by optimally spreading the prediction error over the state space in a least squares sense, rather than near a single point. These models can lead to simple and effective control strategies for high-dimensional nonlinear systems, as demonstrated by Deem et al. (79), who presented a fluid flow experiment in which a separation bubble was suppressed. In particular, they used an online DMD approach to adaptively design linear quadratic regulators that fed surface pressure measurements back to a zero-net mass-flux actuator in a manner that significantly reduced flow separation compared with standard open-loop approaches. The dramatic reduction in the size of the separation bubble in the experimental apparatus using this technique is shown in **Figure 3**.

Low-dimensional linear representations of the dynamics of observables can also be used for estimation. In particular, Surana & Banaszuk (80) leveraged the linear dynamics of nonlinear observables to design a Kalman filter that estimates the values of the observables from measurements that are closely approximated in their span. Gomez et al. (81) later used this so-called Koopman Kalman filter in conjunction with a model identified via sparsity-promoting DMD (34) to estimate the flow field near an airfoil at a near-stall angle of attack from pressure measurements made by sensors on the airfoil's surface.

5. CONCLUDING REMARKS

Koopman operator methods have advanced considerably in recent years. We have reviewed a variety of numerical methods for data-driven approximation of the Koopman operator or generator—for instance, via Galerkin projection onto basis functions that may be chosen from a predetermined

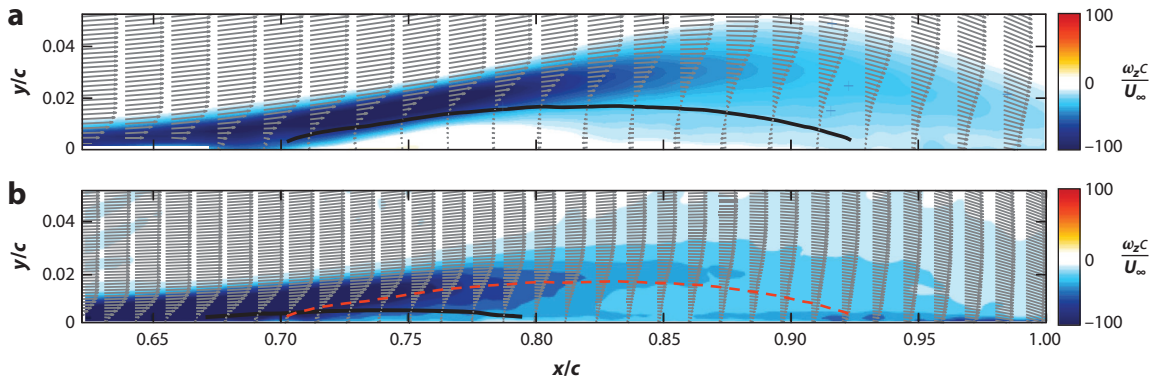

Figure 3

Average velocity field (*arrows*), vorticity (*color*), and sizes of the separation bubble (*black line*) computed from experimental particle image velocimetry. Panel *a* shows the size of the bubble without control, and panel *b* shows the size of the bubble using the online dynamic mode decomposition–based adaptive linear quadratic regulator control strategy. Figure adapted with permission from Reference 79; copyright 2020 Cambridge University Press.

dictionary or learned from data. Below, we summarize some of the main points of this article and point out some outstanding challenges.

SUMMARY POINTS

1. The Koopman and Perron–Frobenius operator viewpoint is concerned with the global aggregate behavior of systems viewed through the lenses of observable functions and probability distributions rather than individual trajectories. This makes these operators especially useful for studying—and potentially controlling—systems that are stochastic or chaotic.
2. For ergodic systems, excellent approximation techniques have been developed for the Koopman generator—for instance, guaranteeing convergence of the spectrum.
3. For systems that are not measure preserving, approximation techniques are also available, although they lack some of the nice spectral convergence properties of the approaches for ergodic systems.
4. If the Koopman operator (or generator) has a finite-dimensional invariant subspace, this may be used to determine coordinates whose evolution is linear and decoupled from other coordinates.
5. Chaotic (e.g., mixing) systems do not have such coordinates, but approximations to the Koopman operator can still be used to produce near-term forecasts.
6. For systems with actuation, the Koopman generator is an especially useful tool, since it is parameterized by the input in essentially the same way as the governing equations.
7. If an actuated system is affine in the control input, then invariant subspaces of the Koopman generator naturally give rise to systems that are bilinear in the state and the control input, plus a linear drift. This structure has been leveraged in a variety of effective control and estimation strategies.

FUTURE ISSUES

1. When using data-driven approximations of the Koopman operator, it can be difficult to tell whether eigenvalues of the approximate operators correspond to actual eigenvalues of the Koopman operator. Improved regularization methods are needed in the non-measure-preserving setting to give better control over the spectrum of the approximate operators.
2. It would be useful to extend some of the numerical methods available for ergodic systems to the transient (off-attractor) setting or to systems with control inputs.
3. Neural networks can be useful for approximating the Koopman operator, but it is not clear whether or in what sense these approaches converge—for instance, as the amount of data and number of artificial neurons tends to infinity.
4. Incorporating actuation into neural network approaches appears to be straightforward and should be attempted on a challenging problem.
5. It would be useful to develop techniques for control synthesis that exploit the special structure of systems that are bilinear in the state and control, plus a linear drift.

DISCLOSURE STATEMENT

The authors are not aware of any affiliations, memberships, funding, or financial holdings that might be perceived as affecting the objectivity of this review.

ACKNOWLEDGMENTS

The authors gratefully acknowledge support from the Army Research Office (award W911NF-17-1-0512), the Air Force Office of Scientific Research (award FA9550-17-1-0084 and Multidisciplinary University Research Initiative award FA9550-19-1-0005), and the National Science Foundation Graduate Research Fellowship Program (award DGE-2039656).

LITERATURE CITED

1. Koopman BO. 1931. Hamiltonian systems and transformations in Hilbert space. *PNAS* 17:315–18
2. von Neumann J. 1932. Proof of the quasi-ergodic hypothesis. *PNAS* 18:70–82
3. Giannakis D. 2019. Data-driven spectral decomposition and forecasting of ergodic dynamical systems. *Appl. Comput. Harmon. Anal.* 47:338–96
4. Reed M, Simon B. 1980. *Methods of Modern Mathematical Physics*, Vol. 1: *Functional Analysis*. San Diego, CA: Academic
5. Mezić I. 2020. Spectrum of the Koopman operator, spectral expansions in functional spaces, and state-space geometry. *J. Nonlinear Sci.* 30:2091–45
6. Lusch B, Kutz JN, Brunton SL. 2018. Deep learning for universal linear embeddings of nonlinear dynamics. *Nat. Commun.* 9:4950
7. Koopman BO, von Neumann J. 1932. Dynamical systems of continuous spectra. *PNAS* 18:255–63
8. Das S, Giannakis D, Slawinska J. 2018. Reproducing kernel Hilbert space compactification of unitary evolution groups. arXiv:1808.01515 [math.DS]
9. Korda M, Putinar M, Mezić I. 2020. Data-driven spectral analysis of the Koopman operator. *Appl. Comput. Harmon. Anal.* 48:599–629
10. Cornfeld IP, Fomin SV, Sinai YG. 1982. *Ergodic Theory*. New York: Springer

11. Pavliotis GA. 2014. *Stochastic Processes and Applications: Diffusion Processes, the Fokker-Planck and Langevin Equations*. New York: Springer
12. Mezić I. 2005. Spectral properties of dynamical systems, model reduction and decompositions. *Nonlinear Dyn*. 41:309–25
13. Froyland G, Gottwald GA, Hammerlindl A. 2014. A computational method to extract macroscopic variables and their dynamics in multiscale systems. *SIAM J. Appl. Dyn. Syst*. 13:1816–46
14. Wu H, Noé F. 2020. Variational approach for learning Markov processes from time series data. *J. Nonlinear Sci*. 30:23–66
15. Lan Y, Mezić I. 2013. Linearization in the large of nonlinear systems and Koopman operator spectrum. *Phys. D* 242:42–53
16. Mauroy A, Mezić I. 2016. Global stability analysis using the eigenfunctions of the Koopman operator. *IEEE Trans. Autom. Control* 61:3356–69
17. Mauroy A, Mezić I. 2012. On the use of Fourier averages to compute the global isochrons of (quasi) periodic dynamics. *Chaos* 22:033112
18. Mauroy A, Mezić I, Moehlis J. 2013. Isostables, isochrons, and Koopman spectrum for the action-angle representation of stable fixed point dynamics. *Phys. D* 261:19–30
19. Dellnitz M, Junge O. 1999. On the approximation of complicated dynamical behavior. *SIAM J. Numer. Anal*. 36:491–515
20. Froyland G, Dellnitz M. 2003. Detecting and locating near-optimal almost-invariant sets and cycles. *SIAM J. Sci. Comput*. 24:1839–63
21. Froyland G, Padberg K, England MH, Treguier AM. 2007. Detection of coherent oceanic structures via transfer operators. *Phys. Rev. Lett*. 98:224503
22. Froyland G. 2013. An analytic framework for identifying finite-time coherent sets in time-dependent dynamical systems. *Phys. D* 250:1–19
23. Froyland G, González-Tokman C, Quas A. 2014. Detecting isolated spectrum of transfer and Koopman operators with Fourier analytic tools. *J. Comput. Dyn*. 1:249–78
24. Schmid PJ. 2010. Dynamic mode decomposition of numerical and experimental data. *J. Fluid Mech*. 656:5–28
25. Rowley CW, Mezić I, Bagheri S, Schlatter P, Henningson DS. 2009. Spectral analysis of nonlinear flows. *J. Fluid Mech*. 641:115–27
26. Williams MO, Kevrekidis IG, Rowley CW. 2015. A data-driven approximation of the Koopman operator: extending dynamic mode decomposition. *J. Nonlinear Sci*. 25:1307–46
27. Brunton SL, Brunton BW, Proctor JL, Kaiser E, Kutz JN. 2017. Chaos as an intermittently forced linear system. *Nat. Commun*. 8:19
28. Williams MO, Rowley CW, Kevrekidis IG. 2015. A kernel-based method for data-driven Koopman spectral analysis. *J. Comput. Dyn*. 2:247–65
29. Klus S, Koltai P, Schütte C. 2016. On the numerical approximation of the Perron-Frobenius and Koopman operator. *J. Comput. Dyn*. 3:51–79
30. Klus S, Nüske F, Koltai P, Wu H, Kevrekidis I, et al. 2018. Data-driven model reduction and transfer operator approximation. *J. Nonlinear Sci*. 28:985–1010
31. Klus S, Nüske F, Peitz S, Niemann JH, Clementi C, Schütte C. 2020. Data-driven approximation of the Koopman generator: model reduction, system identification, and control. *Phys. D* 406:132416
32. Korda M, Mezić I. 2018. On convergence of extended dynamic mode decomposition to the Koopman operator. *J. Nonlinear Sci*. 28:687–710
33. Hemati MS, Rowley CW, Deem EA, Cattafesta LN. 2017. De-biasing the dynamic mode decomposition for applied Koopman spectral analysis of noisy datasets. *Theor. Comput. Fluid Dyn*. 31:349–68
34. Jovanović MR, Schmid PJ, Nichols JW. 2014. Sparsity-promoting dynamic mode decomposition. *Phys. Fluids* 26:024103
35. Li Q, Dietrich F, Bollt EM, Kevrekidis IG. 2017. Extended dynamic mode decomposition with dictionary learning: a data-driven adaptive spectral decomposition of the Koopman operator. *Chaos* 27:103111
36. Goodfellow I, Bengio Y, Courville A. 2016. *Deep Learning*. Cambridge, MA: MIT Press

37. Takeishi N, Kawahara Y, Yairi T. 2017. Learning Koopman invariant subspaces for dynamic mode decomposition. In *Advances in Neural Information Processing Systems 30*, ed. I Guyon, UV Luxburg, S Bengio, H Wallach, R Fergus, et al., pp. 1130–40. Red Hook, NY: Curran
38. Wehmeyer C, Noé F. 2018. Time-lagged autoencoders: deep learning of slow collective variables for molecular kinetics. *J. Chem. Phys*. 148:241703
39. Morton J, Jameson A, Kochenderfer MJ, Witherden F. 2018. Deep dynamical modeling and control of unsteady fluid flows. In *Advances in Neural Information Processing Systems 31*, ed. S Bengio, H Wallach, H Larochelle, K Grauman, N Cesa-Bianchi, R Garnett, pp. 9258–68. Red Hook, NY: Curran
40. Yeung E, Kundu S, Hodas N. 2019. Learning deep neural network representations for Koopman operators of nonlinear dynamical systems. In *2019 American Control Conference*, pp. 4832–39. Piscataway, NJ: IEEE
41. Otto SE, Rowley CW. 2019. Linearly recurrent autoencoder networks for learning dynamics. *SIAM J. Appl. Dyn. Syst*. 18:558–93
42. Pan S, Duraisamy K. 2020. Physics-informed probabilistic learning of linear embeddings of nonlinear dynamics with guaranteed stability. *SIAM J. Appl. Dyn. Syst*. 19:480–509
43. Champion K, Lusch B, Kutz JN, Brunton SL. 2019. Data-driven discovery of coordinates and governing equations. *PNAS* 116:22445–51
44. Chen TQ, Rubanova Y, Bettencourt J, Duvenaud DK. 2018. Neural ordinary differential equations. In *Advances in Neural Information Processing Systems 31*, ed. S Bengio, H Wallach, H Larochelle, K Grauman, N Cesa-Bianchi, R Garnett, pp. 6571–83. Red Hook, NY: Curran
45. Berry T, Giannakis D, Harlim J. 2015. Nonparameteric forecasting of low-dimensional dynamical systems. *Phys. Rev. E* 91:032915
46. Das S, Giannakis D. 2019. Delay-coordinate maps and the spectra of Koopman operators. *J. Stat. Phys*. 175:1107–45
47. Das S, Giannakis D. 2020. Koopman spectra in reproducing kernel Hilbert spaces. *Appl. Comput. Harmon. Anal*. 49:573–607
48. Giannakis D, Kolchinskaya A, Krasnov D, Schumacher J. 2018. Koopman analysis of the long-term evolution in a turbulent convection cell. *J. Fluid Mech*. 847:735–67
49. Coifman RR, Lafon S. 2006. Diffusion maps. *Appl. Comput. Harmon. Anal*. 21:5–30
50. Berry T, Harlim J. 2015. Variable bandwidth diffusion kernels. *Appl. Comput. Harmon. Anal*. 40:68–96
51. Aronszajn N. 1950. Theory of reproducing kernels. *Trans. Am. Math. Soc*. 68:337–404
52. Williams MO, Hemati MS, Dawson ST, Kevrekidis IG, Rowley CW. 2016. Extending data-driven Koopman analysis to actuated systems. *IFAC-PapersOnLine* 49(18):704–9
53. Pazy A. 1983. *Semigroups of Linear Operators and Applications to Partial Differential Equations*. New York: Springer
54. Surana A. 2016. Koopman operator based observer synthesis for control-affine nonlinear systems. In *2016 IEEE 55th Conference on Decision and Control*, pp. 6492–99. Piscataway, NJ: IEEE
55. Mauroy A, Goncalves J. 2016. Linear identification of nonlinear systems: a lifting technique based on the Koopman operator. In *2016 IEEE 55th Conference on Decision and Control*, pp. 6500–5. Piscataway, NJ: IEEE
56. Goswami D, Paley DA. 2017. Global bilinearization and controllability of control-affine nonlinear systems: a Koopman spectral approach. In *2017 IEEE 56th Annual Conference on Decision and Control*, pp. 6107–12. Piscataway, NJ: IEEE
57. Huang B, Ma X, Vaidya U. 2020. Data-driven nonlinear stabilization using Koopman operator. In *The Koopman Operator in Systems and Control: Concepts, Methodologies, and Applications*, ed. A Mauroy, I Mezić, Y Susuki, pp. 313–34. Cham, Switz.: Springer
58. Brockett RW. 1972. System theory on group manifolds and coset spaces. *SIAM J. Control* 10:265–84
59. Proctor JL, Brunton SL, Kutz JN. 2016. Dynamic mode decomposition with control. *SIAM J. Appl. Dyn. Syst*. 15:142–61
60. Korda M, Mezić I. 2018. Linear predictors for nonlinear dynamical systems: Koopman operator meets model predictive control. *Automatica* 93:149–60
61. Korda M, Susuki Y, Mezić I. 2018. Power grid transient stabilization using Koopman model predictive control. *IFAC-PapersOnLine* 51(28):297–302

62. Arbabi H, Korda M, Mezić I. 2018. A data-driven Koopman model predictive control framework for nonlinear partial differential equations. In *2018 IEEE Conference on Decision and Control*, pp. 6409–14. Piscataway, NJ: IEEE
63. Narasingam A, Kwon JSI. 2019. Koopman Lyapunov-based model predictive control of nonlinear chemical process systems. *AIChE J.* 65:e16743
64. Kaiser E, Kutz JN, Brunton SL. 2020. Data-driven approximations of dynamical systems operators for control. In *The Koopman Operator in Systems and Control: Concepts, Methodologies, and Applications*, ed. A Mauroy, I Mezić, Y Susuki, pp. 197–234. Cham, Switz.: Springer
65. Brunton SL, Brunton BW, Proctor JL, Kutz JN. 2016. Koopman invariant subspaces and finite linear representations of nonlinear dynamical systems for control. *PLOS ONE* 11:e0150171
66. Carleman T. 1932. Application de la théorie des équations intégrales linéaires aux systèmes d'équations différentielles non linéaires. *Acta Math*. 59:63–87
67. Kazantzis N, Kravaris C. 1999. Time-discretization of nonlinear control systems via Taylor methods. *Comput. Chem. Eng*. 23:763–84
68. Hashemian N, Armaou A. 2015. Fast moving horizon estimation of nonlinear processes via Carleman linearization. In *2015 American Control Conference*, pp. 3379–85. Piscataway, NJ: IEEE
69. Forets M, Pouly A. 2017. Explicit error bounds for Carleman linearization. arXiv:1711.02552 [math.NA]
70. Steeb WH, Wilhelm F. 1980. Non-linear autonomous systems of differential equations and Carleman linearization procedure. *J. Math. Anal. Appl.* 77:601–11
71. Kowalski K, Steeb WH. 1991. *Nonlinear Dynamical Systems and Carleman Linearization*. Singapore: World Sci.
72. Banks S. 1992. Infinite-dimensional Carleman linearization, the Lie series and optimal control of nonlinear partial differential equations. *Int. J. Syst. Sci.* 23:663–75
73. Peitz S, Otto SE, Rowley CW. 2020. Data-driven model predictive control using interpolated Koopman generators. *SIAM J. Appl. Dyn. Syst*. 19:2162–93
74. Rowley CW, Dawson ST. 2017. Model reduction for flow analysis and control. *Annu. Rev. Fluid Mech*. 49:387–417
75. Zhang H, Dawson ST, Rowley CW, Deem EA, Cattafesta LN. 2019. Evaluating the accuracy of the dynamic mode decomposition. *J. Comput. Dyn*. 7:35–56
76. Wynn A, Pearson D, Ganapathisubramani B, Goulart PJ. 2013. Optimal mode decomposition for unsteady flows. *J. Fluid Mech*. 733:473–503
77. Peitz S, Klus S. 2019. Koopman operator-based model reduction for switched-system control of PDEs. *Automatica* 106:184–91
78. Huang B, Ma X, Vaidya U. 2018. Feedback stabilization using Koopman operator. In *2018 IEEE Conference on Decision and Control*, pp. 6434–39. Piscataway, NJ: IEEE
79. Deem EA, Cattafesta LN, Hemati M, Zhang H, Rowley CW, Mittal R. 2020. Adaptive separation control of a laminar boundary layer using online dynamic mode decomposition. *J. Fluid Mech*. 903:A21
80. Surana A, Banaszuk A. 2016. Linear observer synthesis for nonlinear systems using Koopman operator framework. *IFAC-PapersOnLine* 49(18):716–23
81. Gomez DF, Lagor FD, Kirk PB, Lind AH, Jones AR, Paley DA. 2019. Data-driven estimation of the unsteady flowfield near an actuated airfoil. *J. Guid. Control Dyn*. 42:2279–87